Bifidobacterium breve CBT BR3 is effective in relieving intestinal inflammation by augmenting goblet cell regeneration

Jongwook Yu

Department of Medicine

The Graduate School, Yonsei University

Bifidobacterium breve CBT BR3 is effective in relieving intestinal inflammation by augmenting goblet cell regeneration

Directed by Professor Jae Hee Cheon

The Doctoral Dissertation submitted to the Department of Medicine, the Graduate School of Yonsei University in partial fulfillment of the requirements for the degree of Doctor of Philosophy

Jongwook Yu

December 2021

This certifies that the Doctoral Dissertation of Jongwook Yu is approved.

Thesis Supervisor: Jae Hee Cheon

Thesis Committee Member #1: Tae Il Kim

Thesis Committee Member #2: Seong-Joon Koh

Thesis Committee Member #3: Sang Sun Yoon

Thesis Committee Member #4: Seung Won Kim

The Graduate School
Yonsei University

December 2021

ACKNOWLEDGEMENTS

I would like to express my sincere gratitude to the professors in my thesis committee for the insightful comments, helpful questions and encouragement.

I would like to give my special thanks to Prof. Jae Hee Cheon, my research supervisor, for giving me the opportunity to do research and obtain a degree under his invaluable guidance.

I am very grateful to my parents, wife, son, brother and family for everything.

<TABLE OF CONTENTS>

LIST OF FIGURES

LIST OF TABLES

ABSTRACT

Bifidobacterium breve CBT BR3 is effective in relieving intestinal inflammation by augmenting goblet cell regeneration

Jongwook Yu

Department of Medicine
The Graduate School, Yonsei University

(Directed by Professor Jae Hee Cheon)

Probiotics are microorganisms that have beneficial properties for their hosts. *Bifidobacterium* is an anaerobic, gram-positive, catalase-negative, and rod-shaped bacterium. *Bifidobacterium breve* (*B. breve*) is the first isolated bacteria in the feces of healthy infants and is a dominant species in the guts of breast-fed infants. Some strains of *B. breve* are effective at relieving intestinal inflammation though pathogenesis is not elucidated in detail. In this study, I attempted to elucidate the pathogenesis of *B. breve* CBT BR3 isolated from South Korean infant feces using experimental animal models. *B. breve* CBT BR3 was orally administered to determine its effects as a probiotic on two kinds of murine colitis models. Colitis was induced with dextran sodium sulfate (DSS) and dinitrobenzene sulfonic acid (DNBS), respectively. The disease activity index (DAI) of the mice was recorded. After sacrifice, colon tissues were analyzed for periodic acid-Schiff staining and mRNA expression.

B. breve CBT BR3 improved colitis symptoms as determined by the disease activity index. The DSS-induced colitis mice treated with *B. breve* CBT BR3 had a 62.5% survival rate while the DSS-vehicle group only had a 50% survival rate. Mice in both groups had similar body weights, colon lengths, and colon length-to-initial body weight

ratios. *B. breve* CBT BR3 did not have a significant proliferative effect on goblet cells in normal mucosa but it did increase both goblet cell density and the number of goblet cells per crypt in both groups. In both the DSS- and DNBS-colitis groups, *B. breve* increased mRNA expression of *Spdef* and *Klf4*, genes associated with goblet cell differentiation, and *Muc5*, but not *Muc2*. The mRNA expression of *Occludin*, a membrane tight junction protein, and *Foxo3*, which is related to butyrate metabolism, are also increased. FACS analysis for *Rag1* KO mice showed that *B. breve* may affect through innate lymphoid cells. This study showed that *B. breve* CBT BR3 is effective at relieving intestinal inflammation by augmenting goblet cell regeneration, possibly through innate lymphoid cells and cytokines such as IL-10.

Keywords: inflammatory bowel disease, goblet cells, *Bifidobacterium breve*, probiotics, innate lymphoid cells

Bifidobacterium breve CBT BR3 is effective in relieving intestinal inflammation by augmenting goblet cell regeneration

Jongwook Yu

Department of Medicine
The Graduate School, Yonsei University

(Directed by Professor Jae Hee Cheon)

I. Introduction

Probiotics are microorganisms that have beneficial properties for their hosts.[1-3] They are associated with various human diseases, such as inflammatory bowel diseases (IBD), irritable bowel syndrome, allergic diseases, and even cancers.[1,3-6] Although their pathophysiology is not clearly understood, they seem to have local effects through intestinal mucosa and immune-modulating systemic effects by interacting with their hosts.[7-9] It is impossible to prove each probiotics' pathophysiology because of the intestinal microbiology system's complexity.

IBD is an intestinal disease of unknown etiology, though multiple factors, such as genetic, immunological, and environmental factors, seem to be involved.[10,11] One hypothesis is that an imbalance in commensal bacteria or intestinal microbiome causes abnormal intestinal homeostasis, which in turn causes intestinal mucosal inflammation.[12,13] IBD is managed in various ways, such as with 5-aminosalicylic acids, immunomodulators such as azathioprine and 6-mercaptopurine, corticosteroids, and biological agents, though they all have possibly significant side effects. Probiotics are

another treatment option and are popular because they rarely have side effects, though few studies support their efficacy under real-world conditions.[14] Probiotics have been shown to be effective at reducing intestinal inflammation, especially in patients with UC rather than CD, although this effect is not enough to prove that they are associated with the pathophysiology of IBD.[7,14-26] Although some probiotics may be related to IBD, it is difficult to which specific strains are because there are so many probiotics and microorganisms in mammalian intestines, which can interact in complex ways.[11,14,27-29] The most commonly used and studied probiotics are lactic acid bacilli, including *Lactobacillus* and *Bifidobacterium*.[5,14,30-32] *Bifidobacterium* is an anaerobic, gram-positive, catalase-negative, rod-shaped bacterium that is associated with human diseases.[33-36] *Bifidobacterium breve* (*B. breve*) is one of the first isolated bacteria in the feces of healthy infants and is one of the first colonizers of infant intestines that exhibits antimicrobial activity.[6,37,38] *B. breve* is also a dominant species in the guts of breast-fed infants and has been isolated from human milk and healthy baby feces.[39-41] It may be effective at controlling many diseases, such as obesity, allergic diseases, irritable bowel syndrome (IBS), hypertension, cancer, and even dementia.[4,29,32,42,43] *B. breve* exhibits anti-*Clostridioides difficile* activity in vitro.[44] In 2019, a randomized controlled trial showed that *B. breve* had a protective effect against mucosal injury induced by aspirin in the human small intestine, although its pathophysiology was not shown.[45] In this study, I attempted to identify the pathogenesis of *B. breve* CBT BR3 isolated from South Korean infant feces using experimental animal models.

II. Materials and methods

I studied the effects of *B. breve* CBT BR3 on murine colitis models which were induced with dextran sulfate sodium (DSS) and dinitrobenzene sulfonic acid (DNBS), respectively.

1. Bacterial strains and growth conditions

B. breve CBT BR3, kindly provided by Cell Biotech (Gimpo, South Korea) was cultured in Lactobacilli MRS Broth (BD Difco, NJ, USA) at 37℃ in an incubator and re-suspended in sterile phosphate-buffered saline (PBS) at an optimal concentration.

2. Experiments

C57BL/6 mice were (OrientBio, Sungnam, Gyeonggido, South Korea) received alternating 12 h of light and darkness at 21–22℃ under specific pathogen-free conditions. The mice were administered DSS (MP Biomedicals, Solon, OH, USA) or DNBS (Sigma-Aldrich, St. Louis, MO, USA) to induce colitis. All experiments using animals were reviewed and approved by the Institutional Animal Care and Use Committee of Yonsei University Severance Hospital, Seoul, South Korea (approval no.: 2020-0139) and were conducted in accordance with their guidelines.

A. DSS model

A total of 26 C57BL/6 male mice that were 6–8 weeks old and weighed 20–22 g were selected to serve as DSS-induced colitis models (control: n = 5, *B. breve* CBT BR3 group: n = 5, *B. breve* CBT BR3 with DSS group: n = 8, PBS (vehicle) with DSS group: n = 8). The mice were acclimatized for 1 week before the experiments started. The mice in the treatment group were administered drinking water containing 2.5 % (w/v) DSS from day 0 to day 7 to induce colitis while the mice in the control group were administered untreated drinking water.[46] Mice in the probiotic treatment group were administered 1×10^9 CFU of *B. breve* CBT BR3 in 0.2 mL PBS by oral gavage from day 7 to day 14 after colitis was induced (Fig. 1A).

B. DNBS model

A total of 13 C57BL/6 mice that were 8 weeks old and weighed 20–22 g were selected to serve as DNBS-induced colitis models (DNBS colitis with vehicle group: n = 5, DNBS colitis with *B. breve* CBT BR3: n = 8). Mice were anesthetized using isoflurane (Ifran liquid, Hana Pharm, Seoul, South Korea) in an anesthetic chamber supplemented with sufficient oxygen. Then, 5–6 mg of DNBS/100 ul with 50% ethanol was instilled rectally through an inserted catheter. Then the mice were positioned head-down for 90 s to avoid loss of the DNBS (Fig. 1B).[47]

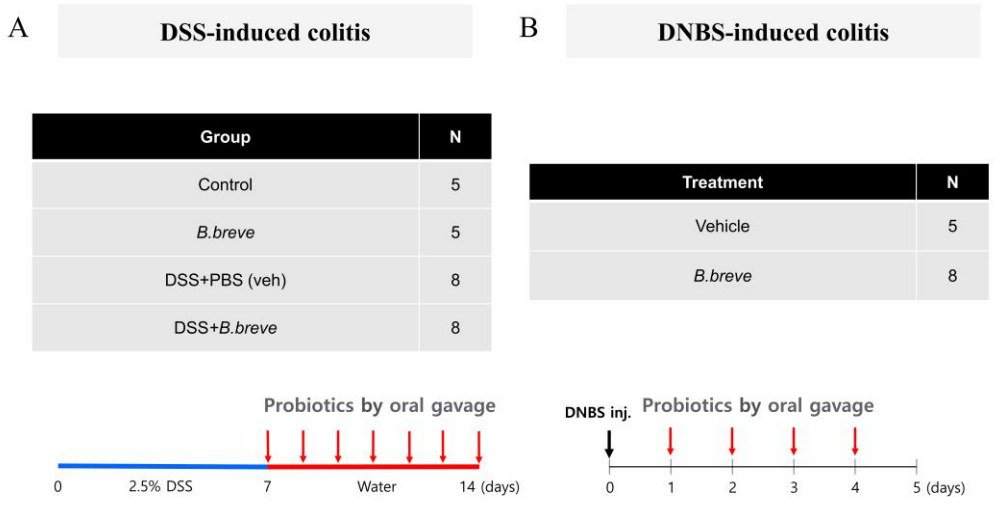

Figure 1. Experimental mouse colitis models.

(A) Male mice that were 6–8 weeks old and weighed 20–22 g were selected to serve as DSS-induced colitis models. The mice in the treatment group were administered drinking water containing 2.5 % (w/v) DSS from day 0 to day 7 to induce colitis while the mice in the control group were administered untreated drinking water. Mice in the probiotic treatment group were administered 1×10^9 CFU of *B. breve* CBT BR3 in 0.2 mL PBS by oral gavage from day 7 to day 14.

(B) A total of 13 C57BL/6 mice that were 8 weeks old and weighed 20–22 g were selected to serve as DNBS-induced colitis models. A catheter was inserted and 5–6 mg of DNBS/100 ul with 50% ethanol was instilled rectally.

The DNBS- and DSS-induced colitis models were completed on days 5 and 14, respectively. The mice were sacrificed with CO_2 gas and their spleens, colons, and entire intestines from the cecum to the anus were collected. Colon length between the cecum and the proximal rectum was measured. The colon was opened and gently cleared of stool using PBS. The distal colon was cut into 2–3 pieces. Then the degree of inflammation and inflammatory marker levels in colon tissue were measured through PAS staining and PCR.

Daily changes in the mice's stool characteristics, such as consistency, frequency, the presence of gross blood in the stool or on the anus; daily activity; body weight; anal protrusions; and overall mortality were recorded. The mice's disease activity indices (DAI) were calculated as the average of their body weight loss, stool consistency, and gross bleeding scores (Table 1). Weight loss was calculated in terms of percentage relative to their weight on day 0.

Table 1. Disease activity index (DAI) scoring system.

Score	A. Body weight change	B. Stool consistency	C. Bleeding
0	None	Normal	None
1	1–5%	Loose	Hemoccult negative
2	5–10%	Loose	Slightly hemoccult positive
3	10–20%	Slight diarrhea	Hemoccult positive
4	> 20%	Watery diarrhea	Gross bleeding

* The calculated DAI score = (A+B+C)/3.

3. Histological analysis

Colon tissue samples were fixed with 10% formalin solution (Biosesang, Seongnam, South Korea) with a pH of 7.4 overnight and then were embedded in paraffin on a slide and sectioned using standard protocols. Deparaffinized sections were subjected to PAS staining using routine techniques for histological examination. Images were obtained with an Olympus BX41 optical microscope (Olympus Optical, Tokyo, Japan). Colitis severity was defined as the sum of the mice's inflammatory cell infiltration and intestinal architecture change scores for a total possible score of 0–8 (Table 2).[48]

PAS-stained slides were imaged and analyzed at x200 magnification. The integrated density (IntDen) of goblet cells in colon tissue was quantified using Image J (National Institutes of Health, Bethesda, MD, USA). IntDen values were obtained from 2–3 random spots on each colon section using the PAS vector of the color deconvolution Image J plugin. The final values were the average of the collected values. Each mouse's number of goblet cells per crypt was the average of 10 randomly chosen intact crypts.

Table 2. Colonic inflammation scoring system.

A. Inflammatory cell infiltrate			**B. Intestinal architecture**		
Severity	Extent	A	**Epithelial changes**	Mucosal architecture	B
Mild	Mucosa	1	**Focal erosions**		1
Moderate	Mucosa or submucosa	2		± Focal ulceration	2
Marked	Transmural	3	**Erosions**	Extended ulceration ± granulation tissue ± Pseudopolyps	3
Death		4	**Death**		4

* The histopathological score = A+B (0–8).

4. Quantitative reverse-transcription polymerase chain reaction

Total RNA was extracted from mouse colons using Ribospin II (GeneAll, Seoul, South Korea) according to the manufacturer's instructions. A High-capacity cDNA Reverse Transcription Kit (Applied Biosystems, CA, USA) was used to reverse-transcribe 1 μg of RNA according to the manufacturer's protocol. Real-time PCR was conducted by mixing cDNA with SYBR Green Master Mix (Applied Biosystems) and pairs of primers. Samples were amplified in a StepOne Plus real-time PCR system (Applied Biosystems) for 45 cycles and subject to the thermal cycler protocol at 95℃ for 30 s, 58–61℃ for 30 s, and 72℃ for 40 s. *β-actin* was used as the endogenous control gene for normalization. *β-actin*, *Muc2*, tissue necrosis factor-alpha (*Tnf-α*), *Klf4*, and *others* were used as primers for real-time PCR (Table 3). Gene expression levels were calculated using the relative comparative method using the following equation:

$$\Delta Ct = Ct_{\text{target gene}} - Ct_{\text{reference gene}}$$

where Ct_i is the number of *i* genes. Relative gene expression levels were calculated using the following equation:

$$\text{Relative expression level} = 2 - \Delta Ct_{sample} - \Delta Ct_{control}$$

Table 3. Real-time PCR primers.

Organism: Mouse		
Gene	**Primer 1 (5'-3')**	**Primer 2 (5'-3')**
β-actin	AGTGTGACGTTGACATCCGT	TGCTAGGAGCCAGAGCAGTA
Muc2	GGTCCAGGGTCTGGATCACA	GCTCAGCTCACTGCCATCTG
Tnfa	CAAAGGGAGAGTGGTCAGGT	ATTGCACCTCAGGGAAGAGT
Klf4	AGAGGAGCCCAAGCCAAAGAGG	CCACAGCCGTCCCAGTCACAGT
Il10	TGAATTCCCTGGGTGAGAAG	TCACTCTTCACCTGCTCCACT
Wnt3a	CATGCACCTCAAGTGCAAATG	TGAGGAAATCCCCGATGGT
Notch1	GCTGCCTCTTTGATGGCTTCGA	CACATTCGGCACTGTTACAGCC
Spdef	AAGGCAGCATCAGGAGCAATG	CTGTCAATGACGGGACACTG
Foxo3	AGCCGTGTACTGTGGAGCTT	TCTTGGCGGTATATGGGAAG
Il13	AGCATGGTATGGAGTGTGGACCTG	CAGTTGCTTTGTGTAGCTGAGCAG
Il33	TCCAACTCCAAGATTTCCCCG	CATGCAGTAGACATGGCAGAA
Occludin	CTCTCAGCCAGCGTACTCTT	CTCCATAGCCACCTCCGTAG
Muc5ac	GAGGCCAACAAGGTAGAGCACA	TGGGACAGCAGCAGTATTCAGT
Organism: Human		
Occludin	TTTGTGGGACAAGGAACACA	TCATTCACTTTGCCATTGGA
Klf4	CGGACATCAACGACGTGAG	GACGCCTTCAGCACGAACT
Muc2	AGGATGACACCATCTACCTCACC	GGTGTAGGCATCGCTCTTCTC

5. Fluorescence-activated cell sorting

A total of 4 male 9-week-old mice were administered 1×10^9 CFU of *B. breve* CBT BR3 in 0.2 mL PBS per day by oral gavage for 6 days. *Rag1* KO mice spleens were dissected and splenocyte suspensions were prepared from them. Flow cytometric analysis of innate lymphoid cells (ILC) was conducted by blocking them with 2.5% normal mouse and rat serum in a fluorescence-activated cell sorting (FACS) buffer of DPBS containing 0.1% BSA and staining with the following antibodies as appropriate: anti-Cd3(eFlour 450), anti-Cd25 (PerCP-Cy5.5), anti-Cd127 (PE-Cy7), and anti-Rorgt (APC). Data was acquired using a FACSVerse flow cytometer (BD Biosciences) and analyzed using FlowJo software (Three Star, San Carlos, CA, USA).

6. In vitro Caco-2 FITC-dextran flux permeability assay

The flux of FITC-dextran was measured to evaluate the integrity of tight junction barriers in Caco-2 cells taken from a human colon adenocarcinoma cell line. Caco-2 cells were seeded in the upper chamber of 12-well transwell chambers and cultured in complete Dulbecco's Modified Eagle Medium (DMEM) (HyClone, UT, USA) containing 10% FBS and 1% Penicillin-Streptomycin at 37 ℃ in a humidified atmosphere of 5% CO2 in air. Then, 200 μl of 1 mg/ml FITC-dextran was added to upper chamber. After 2 h, medium from the lower chamber was collected and its fluorescence was measured using a fluorescent microplate reader. Total RNA from transwell epithelial cells was extracted and 1 μg of RNA was reverse-transcribed. Real-time PCR was conducted by mixing cDNA with pairs of primers. Samples were amplified for 45 cycles and subject to the thermal cycler protocol at 95℃ for 30 sec, 58–61°C for 30 sec, and 72℃ for 40 sec. β-actin was used as the endogenous control gene for normalization. Finally, gene expression levels were calculated.

7. Statistical analysis

The results were examined using GraphPad Prism Software (La Jolla, CA, USA). Statistical significance was assessed using either a Mann-Whitney U test or one-way analysis of variance (ANOVA) with Tukey's posttest. *P*-values < 0.05 were regarded to be statistically significant.

8. Reagents

Bifidobacterium breve CBT BR3 (Cell Biotech, Gimpo, South Korea)
Lactobacilli MRS Broth (BD Difco, NJ, USA)
Phosphate-buffered saline (PBS) (GenDEPOT, TX, USA)
Dextran Sulfate Sodium Salt (DSS) (MP Bio, California, USA)
Dinitrobenzene sulfonic acid (DNBS) (Sigma-Aldrich, St. Louis, MO, USA)
Isoflurane (Ifran Liquid, Hana Pharm, Seoul, South Korea)
10% neutral buffered formalin (Biosesang, Seongnam, South Korea)
Ribospin II (GeneAll, Seoul, South Korea)
High-capacity cDNA reverse transcription kit (Applied Biosystems, CA, USA)
Power SYBR Green PCR Master Mix (Applied Biosystems)
StepOne Plus real-time PCR system (Applied Biosystems)
12 mm transwell with 0.4-μm pore polyester membrane insert (CLS3460)
Fluorescein isothiocyanate-dextran (FD4)
Dulbecco's Modified Eagle Medium, FBS, penicillin-streptomycin
Fluorescent microplate reader

III. Results

1. DAI in DSS-induced colitis models

The DAI for DSS-induced colitis models that were administered *B. breve* CBT BR3 decreased more than that for the DSS-vehicle group meaning that *B. breve* improved colitis symptom in DSS-induced colitis models (Figure 2).

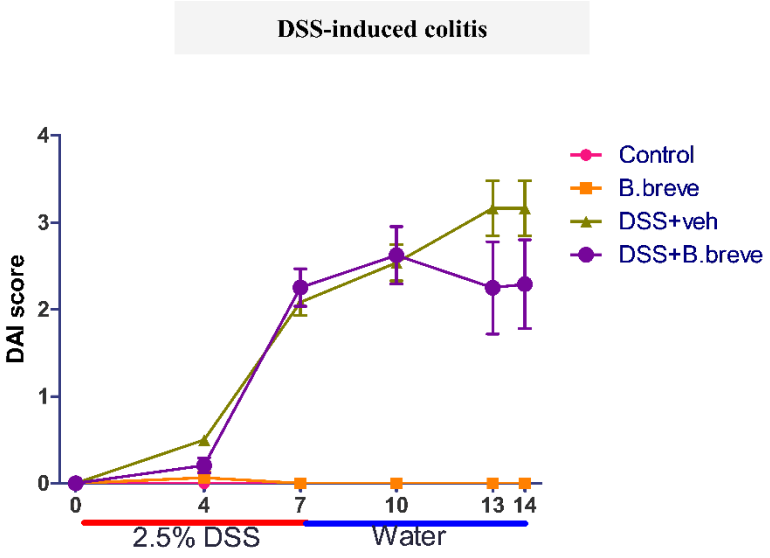

Figure 2. DAIs in DSS-induced colitis models.

Male mice that were 6–8 weeks old and weighed 20–22 g were selected to serve as DSS-induced colitis models. The mice in the treatment group were administered drinking water containing 2.5 % (w/v) DSS from day 0 to day 7 to induce colitis. Mice in the probiotic treatment group were administered 1×10^9 CFU of *B. breve* CBT BR3 in 0.2 mL PBS by oral gavage from day 7 to day 14. Daily changes in the mice were recorded and their DAIs were calculated. On day 14, the mice in the DSS group were sacrificed and their spleens and colons were collected.

* $P < 0.05$, ** $P < 0.01$, *** $P < 0.005$. Analyses were performed using a Mann-Whitney U test or a one-way ANOVA with Tukey's posttest.

2. DAI in DNBS-induced colitis models

The DAI of the DNBS-induced colitis group did not decrease more than that of the DNBS-vehicle group meaning that *B. breve* did not improve colitis symptom in DNBS-induced colitis models (Fig. 3).

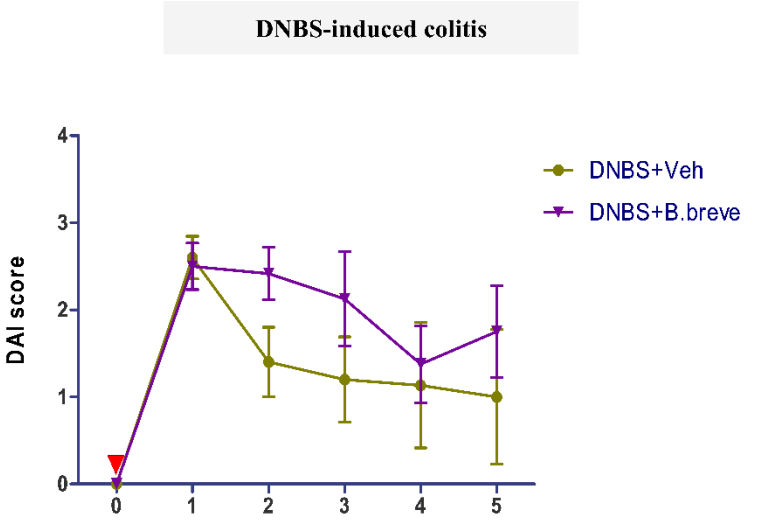

Figure 3. DAIs in DNBS-induced colitis models.

For the DNBS colitis experiment, 8-week-old C57BL/6 mice that weighed 20–22 g were administered 5–6mg of DNBS/100 μl with 50% ethanol rectally through a catheter. Then they were administered either 1×10^9 bacteria or PBS by oral gavage daily for 4 days. Daily changes in the mice were recorded and their DAIs were calculated. On day 5, the mice in the DNBS group were sacrificed and their spleens and colons were collected.

* $P < 0.05$, ** $P < 0.01$, *** $P < 0.005$. Analyses were performed using Mann-Whitney U test or a one-way ANOVA with Tukey's posttest.

3. Body weight change in DSS-induced colitis models

The weight of DSS-vehicle group decreased more than that of DSS colitis group administered with *B. breve* (Fig. 4). *B. breve* significantly preserved body weight in DSS-induced colitis group.

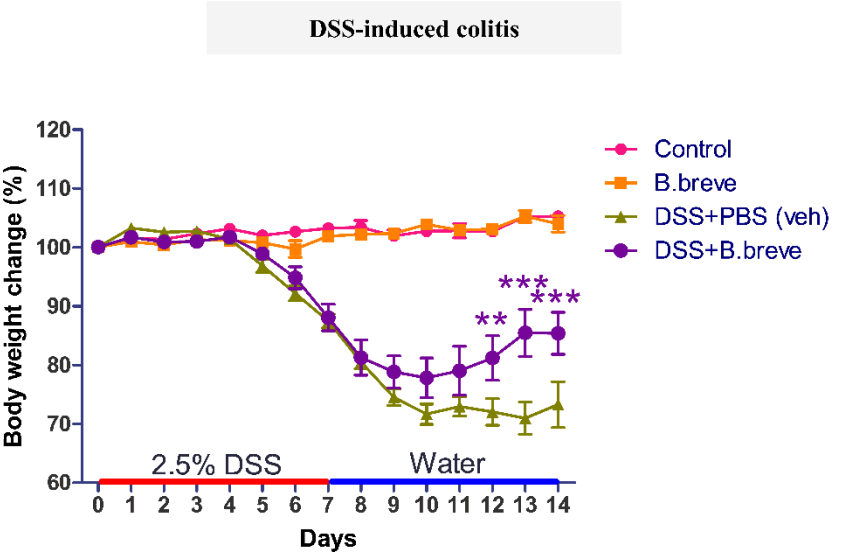

Figure 4. Serial body weight changes in DSS-induced colitis models.

Male mice that were 6–8 weeks old and weighed 20–22 g were selected to serve as DSS-induced colitis models. The mice in the treatment group were administered drinking water containing 2.5 % (w/v) DSS from day 0 to day 7 to induce colitis. Then they were administered 1×10^9 CFU of *B. breve* CBT BR3 in 0.2 mL PBS by oral gavage from day 7 to day 14. Daily changes in the mice were recorded and their DAIs were calculated. On day 14, the mice in the DSS group were sacrificed and their spleens and colons were collected.

* $P < 0.05$, ** $P < 0.01$, *** $P < 0.005$. Analyses were performed using a Mann-Whitney U test or a one-way ANOVA with Tukey's posttest.

4. Body weight change in DNBS-induced colitis models

The DNBS-induced murine colitis group's and the DNBS-vehicle control group's body weights decreased to similar degrees (Fig. 5).

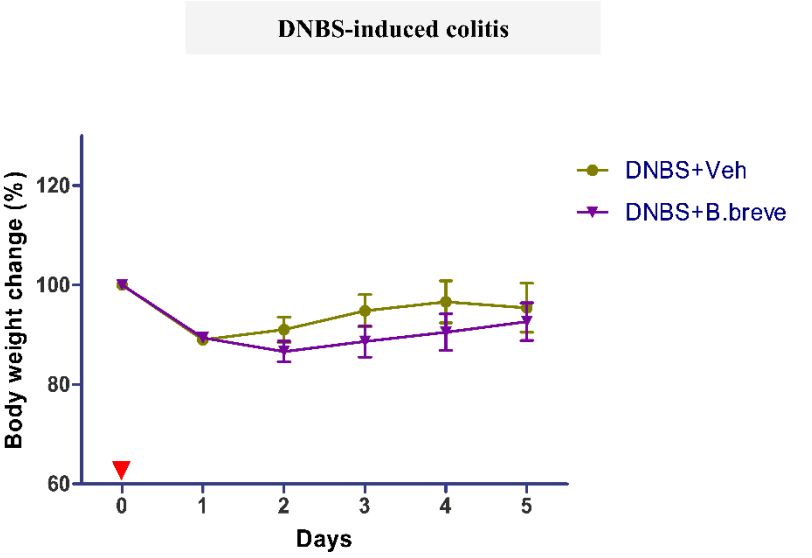

Figure 5. Serial body weight changes in DNBS-induced colitis models.

For the DNBS colitis experiment, 8-week-old C57BL/6 mice that weighed 20–22 g were administered 5–6mg of DNBS/100 μl with 50% ethanol rectally through a catheter. Then they were administered either 1×10^9 bacteria or PBS by oral gavage daily for 4 days. Daily changes in the mice were recorded and their DAIs were calculated. On day 5, the mice in the DNBS group were sacrificed and their spleens and colons were collected.

* $P < 0.05$, ** $P < 0.01$, *** $P < 0.005$. Analyses were performed using a Mann-Whitney U test or a one-way ANOVA with Tukey's posttest.

5. Survival rates in DSS-induced colitis models

In the *B. breve* CBT BR3 group, 5 of the 8 (62.5%) mice survived, but 4 of the 8 (50%) in the DSS-vehicle group survived (Fig. 6). *B. breve* administration improved survival rates in DSS-induced colitis models.

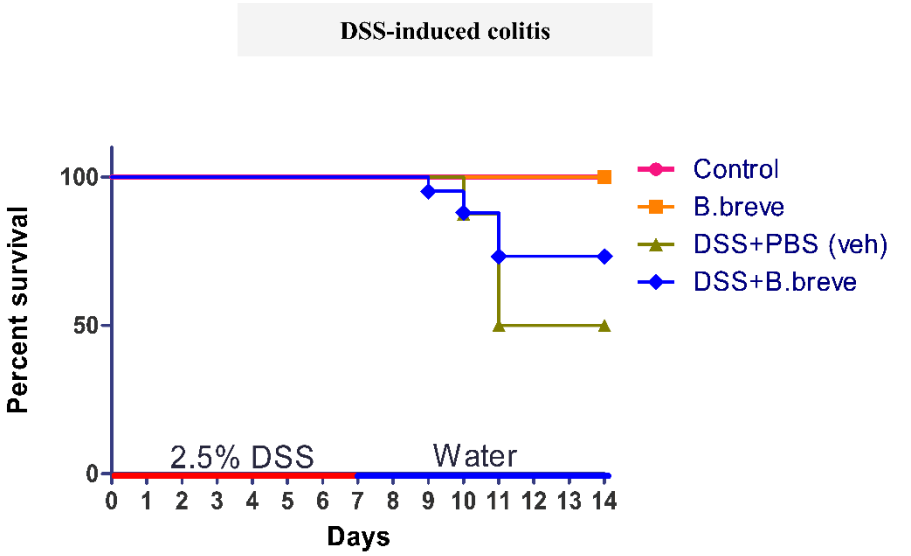

Figure 6. Survival rates in DSS-induced colitis models.

Male mice that were 6–8 weeks old and weighed 20–22 g were selected to serve as DSS-induced colitis models. The mice in the treatment group were administered drinking water containing 2.5 % (w/v) DSS from day 0 to day 7 to induce colitis. Then they were administered 1×10^9 CFU of *B. breve* CBT BR3 in 0.2 mL PBS by oral gavage from day 7 to day 14. Daily changes in the mice were recorded and their DAIs were calculated. On day 14, the mice in the DSS group were sacrificed and their spleens and colons were collected.

* $P < 0.05$, ** $P < 0.01$, *** $P < 0.005$. Analyses were performed using a Mann-Whitney U test or a one-way ANOVA with Tukey's posttest.

6. Survival rates in DNBS-induced colitis models

All of the mice in both the DNBS-vehicle and DNBS-*B. breve* groups survived until day 5 (Fig. 7).

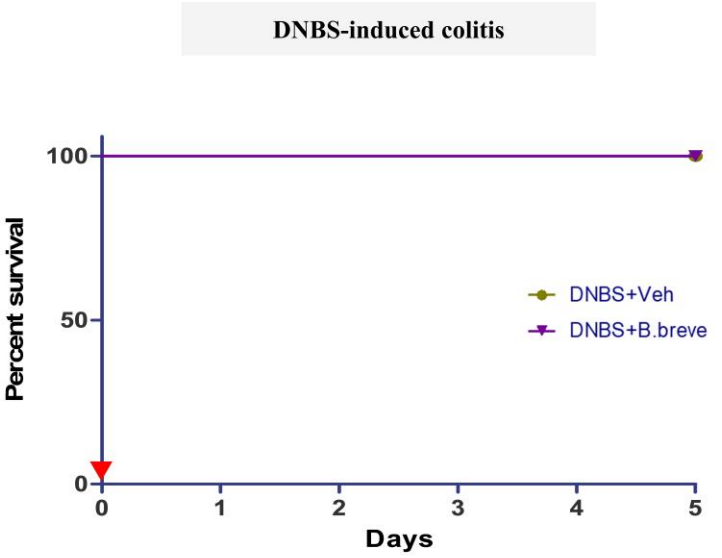

Figure 7. Survival rates in DNBS-induced colitis models.

For the DNBS colitis experiment, 8-week-old C57BL/6 mice that weighed 20–22 g were administered 5–6 mg of DNBS/100 μl with 50% ethanol rectally through a catheter. Then they were administered either 1×10^9 bacteria or PBS by oral gavage daily for 4 days. Daily changes in the mice were recorded and their DAIs were calculated. On day 5, the mice in the DNBS group were sacrificed and their spleens and colons were collected.

*$P < 0.05$, ** $P < 0.01$, *** $P < 0.005$. Analyses were performed using a Mann-Whitney U test or a one-way ANOVA with Tukey's posttest.

7. Colon changes in DSS-induced colitis groups

The *B. breve* group's colon length and colon length-to-initial body weight ratio decreased significantly less than those of the DSS-vehicle colitis group (Fig. 8). *B. breve* administration significantly prevented shortening of colon length and colon length/initial body weight compared to DSS-vehicle colitis group.

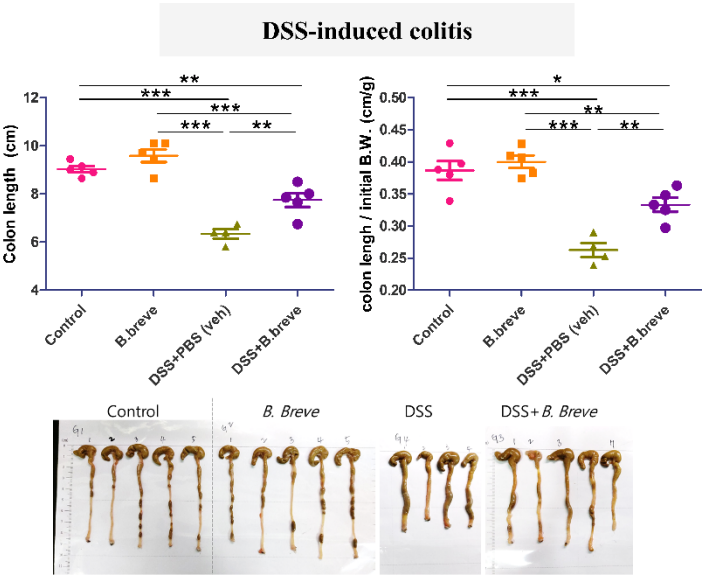

Figure 8. Colon lengths and colon length-to-initial body weight ratios in DSS-induced colitis models.

Male mice that were 6–8 weeks old and weighed 20–22 g were selected to serve as DSS-induced colitis models. The mice in the treatment group were administered drinking water containing 2.5 % (w/v) DSS from day 0 to day 7 to induce colitis. Then they were administered 1×10^9 CFU of *B. breve* CBT BR3 in 0.2 mL PBS by oral gavage from day 7 to day 14. Daily changes in the mice were recorded and their DAIs were calculated. On day 14, the mice in the DSS group were sacrificed and their spleens and colons were collected. The colon lengths were measured from the cecum to the proximal rectum. The colon was opened and gently cleared of stool using PBS. The distal colon was cut into 2–3 pieces for PAS staining and RNA isolation.

* $P < 0.05$, ** $P < 0.01$, *** $P < 0.005$. Analyses were performed using a Mann-Whitney U test or a one-way ANOVA with Tukey's posttest.

8. Colon changes in DNBS-induced colitis groups

There was no statistically significant difference in the colon lengths and colon length-to-initial body weight ratios of the DNBS-vehicle and DNBS-*B. breve* groups (Fig. 9).

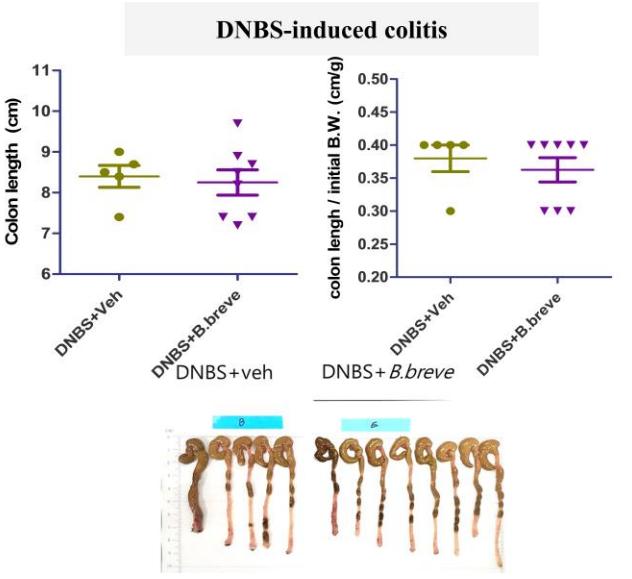

Figure 9. Colon lengths and colon length-to-initial body weight ratios in DNBS-induced colitis models.

For the DNBS colitis experiment, 8-week-old C57BL/6 mice that weighed 20–22 g were administered 5–6 mg of DNBS/100 μl with 50% ethanol rectally through a catheter. Then they were administered either 1×10^9 bacteria or PBS by oral gavage daily for 4 days. Daily changes in the mice were recorded and their DAIs were calculated. On day 5, the mice in the DNBS group were sacrificed and their spleens and colons were collected. The colon lengths were measured from the cecum to the proximal rectum. The colon was opened and gently cleared of stool using PBS. The distal colon was cut into 2–3 pieces for PAS staining and RNA isolation.

* $P < 0.05$, ** $P < 0.01$, *** $P < 0.005$. Analyses were performed using a Mann-Whitney U test or a one-way ANOVA with Tukey's posttest.

9. Histopathological scores in DSS-induced colitis models

The DSS-*B. breve* group had lower histopathological scores than the DSS-vehicle colitis group, but this difference was not statistically significant (Fig. 10). Histopathological scores between proximal colon and distal colon were not significantly different.

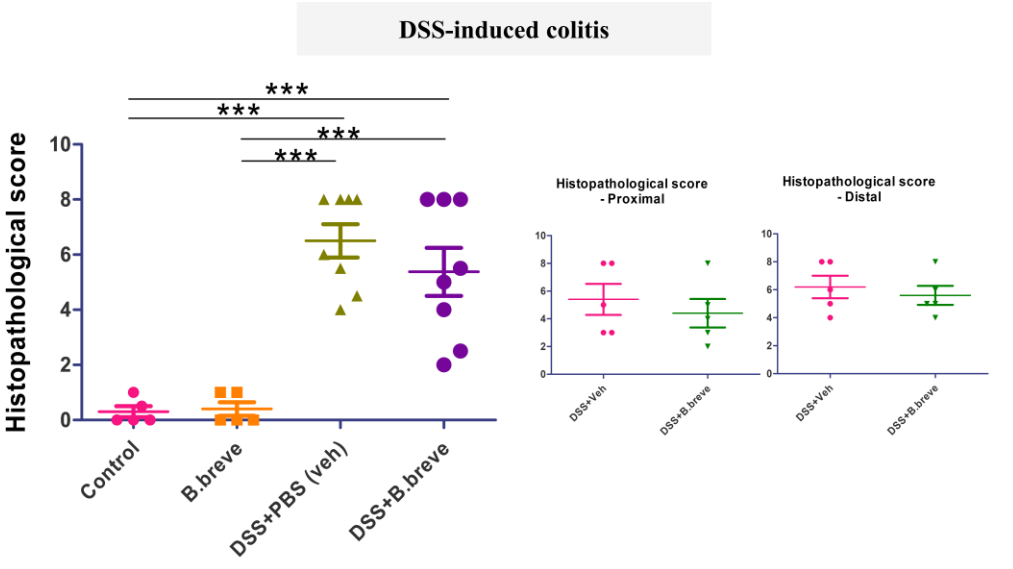

Figure 10. Histopathological scores in DSS-induced colitis models.

Male mice that were 6–8 weeks old and weighed 20–22 g were selected to serve as DSS-induced colitis models. The mice in the treatment group were administered drinking water containing 2.5 % (w/v) DSS from day 0 to day 7 to induce colitis. Then they were administered 1×10^9 CFU of *B. breve* CBT BR3 in 0.2 mL PBS by oral gavage from day 7 to day 14. Daily changes in the mice were recorded and their DAIs were calculated. On day 14, the mice in the DSS group were sacrificed and their spleens and colons were collected. The distal colon was cut into 2–3 pieces for periodic acid-Schiff staining and RNA isolation. Colitis severity was scored according to the extent of inflammatory cell infiltration and intestinal architecture changes.

* $P < 0.05$, ** $P < 0.01$, *** $P < 0.005$. Analyses were performed using a Mann-Whitney U test or a one-way ANOVA with Tukey's posttest.

10. Histopathological scores in DNBS-induced colitis models

Both the DNBS-*B.breve* and DNBS-vehicle colitis groups had similar histopathological scores (Fig. 11).

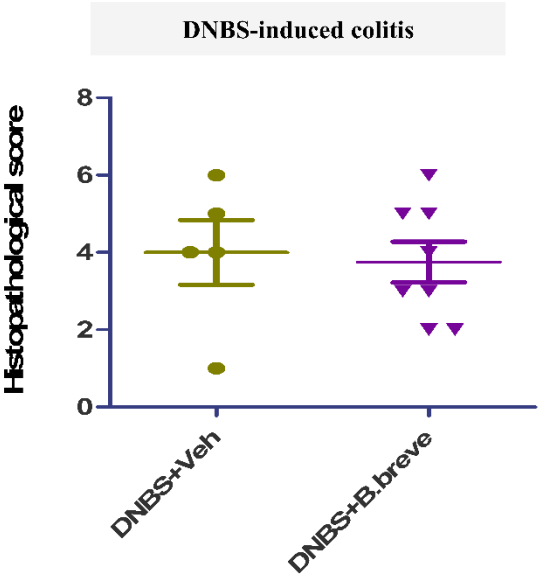

Figure 11. Histopathological scores in DNBS-induced colitis models.

For the DNBS colitis experiment, 8-week-old C57BL/6 mice that weighed 20–22 g were administered 5–6 mg of DNBS/100 μl with 50% ethanol rectally through a catheter. Then they were administered either 1×10^9 bacteria or PBS by oral gavage daily for 4 days. Daily changes in the mice were recorded and their DAIs were calculated. On day 5, the mice in the DNBS group were sacrificed and their spleens and colons were collected. The distal colon was cut into 2–3 pieces for periodic acid-Schiff staining and RNA isolation. Colitis severity was scored according to the extent of inflammatory cell infiltration and intestinal architecture changes.

* $P < 0.05$, ** $P < 0.01$, *** $P < 0.005$. Analyses were performed using a Mann-Whitney U test or a one-way ANOVA with Tukey's posttest.

11. Goblet cell density and numbers in DSS-induced colitis groups

Intestinal goblet cell numbers were assessed in terms of goblet cell density (Fig. 12A) and goblet cell numbers per crypt (Fig. 12B). *B. breve* did not affect goblet cell proliferation in normal mucosa. There were more goblet cells in DSS-treated group mucosa than that of the control or *B. breve* groups. Furthermore, goblet cell density was higher in the group that received *B. breve* than the DSS-induced colitis groups. The results indicated that goblet cells recovered in mucosa injured by DSS during days 1–7 during days 7–14 in the groups that were administered *B. breve*, likely because it helped them differentiate well (Fig.12).

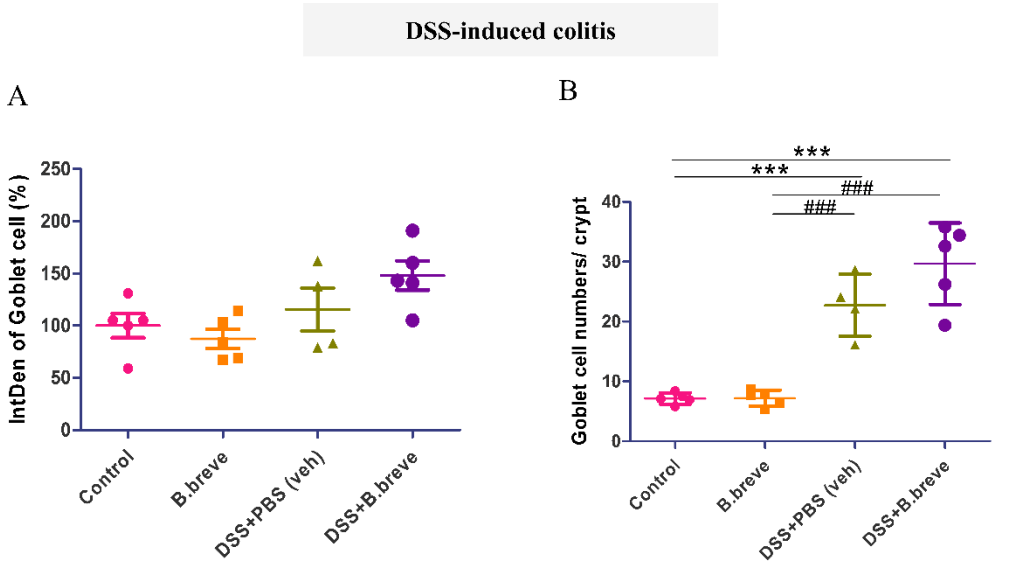

Figure 12. Goblet cell densities and numbers in DSS-induced colitis models.

Male mice that were 6–8 weeks old and weighed 20–22 g were selected to serve as DSS-induced colitis models. The mice in the treatment group were administered drinking water containing 2.5 % (w/v) DSS from day 0 to day 7 to induce colitis. Then they were administered 1×10^9 CFU of *B. breve* CBT BR3 in 0.2 mL PBS by oral gavage from day 7 to day 14. Daily changes in the mice were recorded and their DAIs were calculated. On day 14, the mice in the DSS group were sacrificed and their spleens and colons were collected. The distal colon was cut into 2–3 pieces for PAS staining and RNA isolation. PAS-stained slides were imaged and analyzed at ×200 magnification. The goblet cells' IntDen was determined by Image J software. IntDen values were the average values of random places of each colon section of 2–3 samples determined using the PAS vector of the Image J color deconvolution plugin. Goblet cell counts were the average of the number of goblet cells found in 10 randomly chosen intact crypts per mouse.

* $P < 0.05$, ** $P < 0.01$, *** $P < 0.005$. Analyses were performed using a Mann-Whitney U test or a one-way ANOVA with Tukey's posttest.

12. Goblet cell density and numbers in DNBS-induced colitis groups

Intestinal goblet cell numbers were assessed in terms of goblet cell density and the number of goblet cells per crypt, both of which increased in the group that was administered *B. breve* than in the DNBS-induced colitis group (Fig. 13).

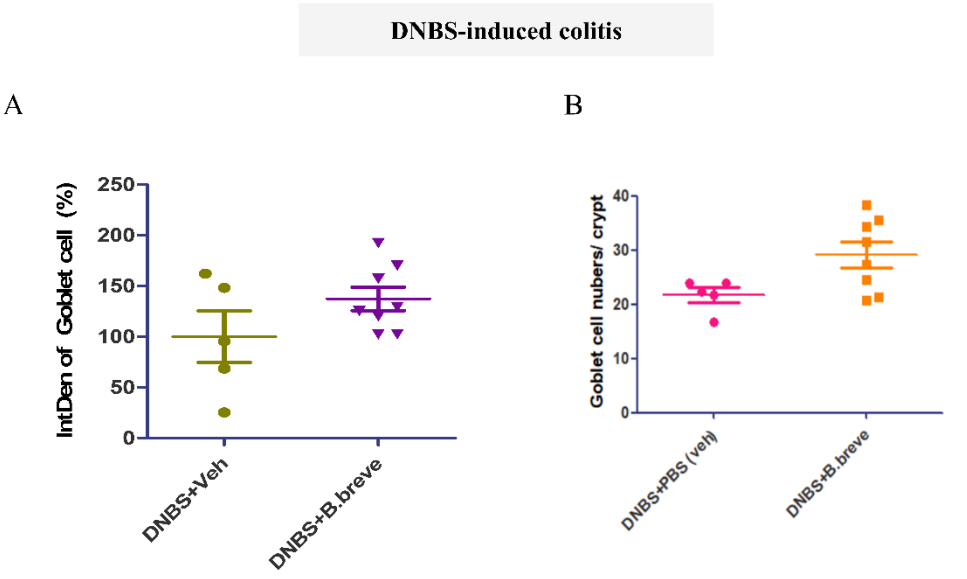

Figure 13. Goblet cell densities and numbers in DNBS-induced colitis models.

For the DNBS colitis experiment, 8-week-old C57BL/6 mice that weighed 20–22 g were administered 5–6 mg of DNBS/100 μl with 50% ethanol rectally through a catheter. Then they were administered either 1×10^9 bacteria or PBS by oral gavage daily for 4 days. Daily changes in the mice were recorded and their DAIs were calculated. On day 5, the mice in the DNBS group were sacrificed and their spleens and colons were collected. The distal colon was cut into 2–3 pieces for periodic acid-Schiff staining and RNA isolation. PAS-stained slides were imaged and analyzed at ×200 magnification. The goblet cells' IntDen was determined by Image J software. IntDen values were the average values of random places of each colon section of 2–3 samples in each colon section determined using the PAS vector of the Image J color deconvolution plugin. Goblet cell counts were the average of the number of goblet cells found in 10 randomly chosen intact crypts per mouse.

* $P < 0.05$, ** $P < 0.01$, *** $P < 0.005$. Analyses were performed using a Mann-Whitney U test or a one-way ANOVA with Tukey's posttest.

13. Histopathological analysis in DSS-induced colitis models

B. breve did not have proliferative effects on normal mucosa. There was no significant difference between the control group and the *B. breve* group in terms of bowel wall thickness, deformity, or inflammation. The DSS-vehicle group exhibited severe inflammatory changes and thickened and deformed intestinal walls, but these changes were ameliorated in the DSS-*B. breve* group. PAS staining showed that the DSS-*B. breve* group had more goblet cells than the DSS-vehicle group (Fig. 14).

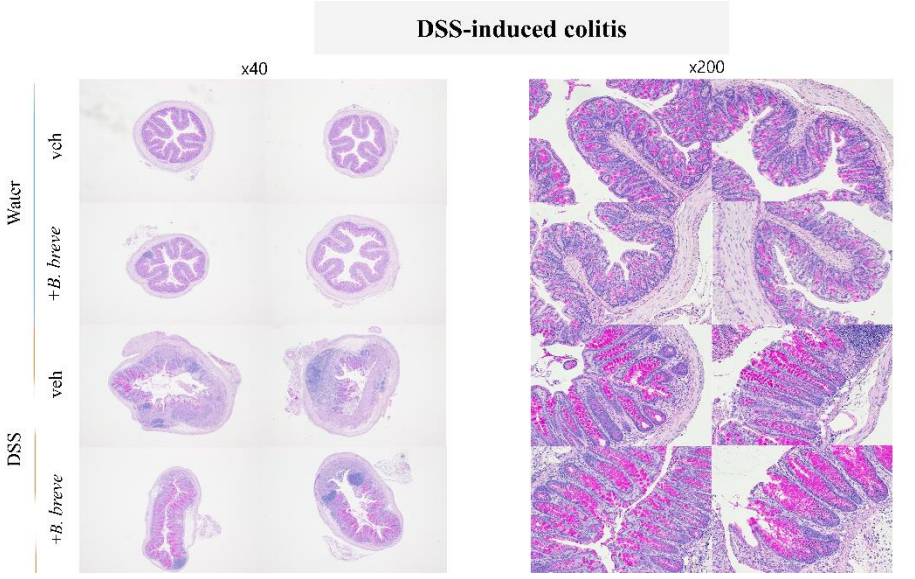

Figure 14. PAS-staining in DSS-induced colitis models.

Male mice that were 6–8 weeks old and weighed 20–22 g were selected to serve as DSS-induced colitis models. The mice in the treatment group were administered drinking water containing 2.5 % (w/v) DSS from day 0 to day 7 to induce colitis. Then they were administered 1×10^9 CFU of *B. breve* CBT BR3 in 0.2 mL PBS by oral gavage from day 7 to day 14. Daily changes in the mice were recorded and their DAIs were calculated. On day 14, the mice in the DSS group were sacrificed and their spleens and colons were collected. The distal colon was cut into 2–3 pieces for PAS staining and RNA isolation. Colon tissue samples were fixed with 10% formalin solution overnight, embedded in paraffin on a slide, and sectioned. Deparaffinized sections were subjected to PAS staining for histological examination and images were obtained with the light microscope. Colitis severity was determined by the extent of inflammatory cell infiltration and intestinal architecture change. PAS-stained slides were imaged and analyzed at magnifications of ×40 and ×200, respectively.

* $P < 0.05$, ** $P < 0.01$, *** $P < 0.005$. Analyses were performed using a Mann-Whitney U test or a one-way ANOVA with Tukey's posttest

14. Histopathological analysis in DNBS-induced colitis models

Although there was no normal control in the DNBS experiments, the samples' histopathologic scores indicated mild to moderate inflammatory changes and intestinal wall thickness and deformity were not significantly different between the DNBS-vehicle and DNBS-*B. breve* groups. Visual inspection of PAS-staining images indicated that the DNBS-*B. breve* group had more goblet cells than the DNBS-vehicle group (Fig. 15).

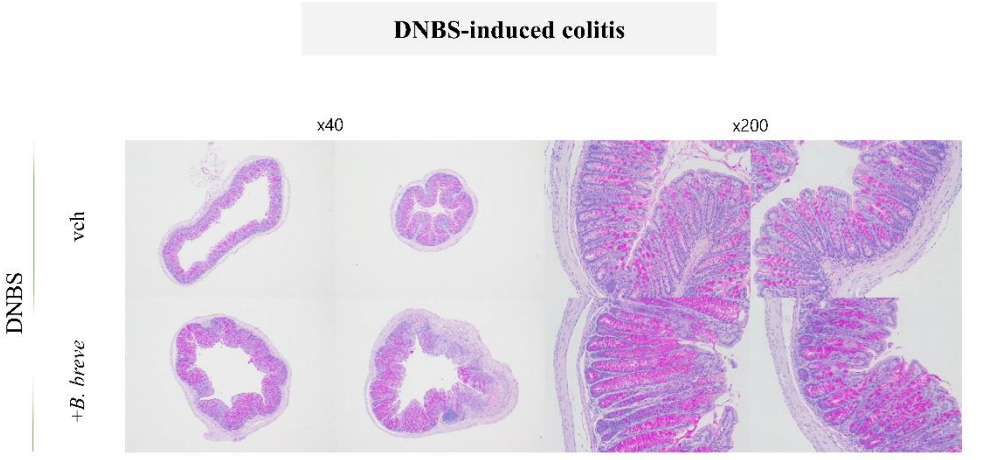

Figure 15. PAS-staining in DNBS-induced colitis models.

For the DNBS colitis experiment, 8-week-old C57BL/6 mice that weighed 20–22 g were administered 5–6mg of DNBS/100 μl with 50% ethanol rectally through a catheter. Then they were administered either 1×10^9 bacteria or PBS by oral gavage daily for 4 days. Daily changes in the mice were recorded and their DAIs were calculated. On day 5, the mice in the DNBS group were sacrificed and their spleens and colons were collected. The distal colon was cut into 2–3 pieces for periodic acid-Schiff staining and RNA isolation. Colon tissue samples were fixed with 10% formalin solution overnight, embedded in paraffin on a slide, and sectioned. Deparaffinized sections were subjected to PAS staining for histological examination and images were obtained with an optical microscope. Colitis severity was determined by the extent of inflammatory cell infiltration and intestinal architecture change. PAS-stained slides were imaged and analyzed at magnifications of x40 and x200, respectively.

* $P < 0.05$, ** $P < 0.01$, *** $P < 0.005$. Analyses were performed using a Mann-Whitney U test or a one-way ANOVA with Tukey's posttest.

15. mRNA expression in DSS-induced colitis models

Real-time PCR was performed to understand the genetic etiology of *B. breve* involved in DSS-induced colitis models (Fig. 16). The expressions of *Notch*, *Wnt3*, and the anti-inflammatory cytokine IL-10 were greater in the DSS-*B. breve* group than in the DSS-vehicle group. This result may have been a non-specific response to intestinal injuries caused by DSS. The expressions of *Spdef* and *Klf4*, which are associated with the terminal differentiation of goblet cells, were higher in the DSS-*B. breve* group than in the DSS-vehicle group. The expression of *Muc2*, which is associated with mucin secretion by goblet cells, was not higher in the DSS-*B. breve* group than in the DSS-vehicle group. Instead of *Muc2*, the expression of *Muc5*, which is also associated with mucin secretion was higher in the DSS-*B. breve* group than in the DSS-vehicle group. In addition, IL-13 expression was higher in the DSS-*B. breve* group than in the DSS-vehicle group while IL-33 expression was not. *Foxo3* expression was higher in the DSS-*B. breve* group than in the DSS-vehicle group.

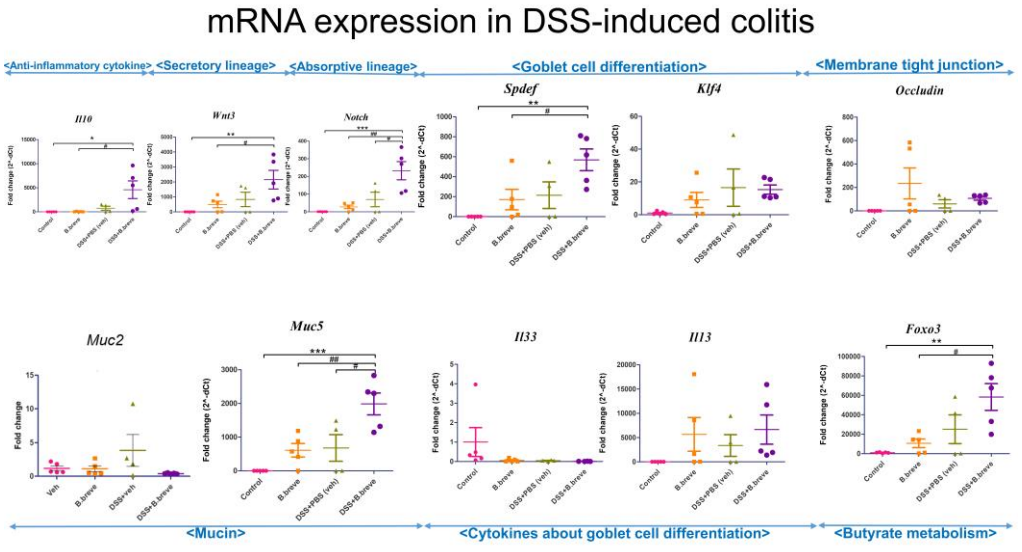

Figure 16. mRNA expression analysis in DSS-induced colitis models.

Male mice that were 6–8 weeks old and weighed 20–22 g were selected to serve as DSS-induced colitis models. The mice in the treatment group were administered drinking water containing 2.5 % (w/v) DSS from day 0 to day 7 to induce colitis. Then they were administered 1×10^9 CFU of *B. breve* CBT BR3 in 0.2 mL PBS by oral gavage from day 7 to day 14. Daily changes in the mice were recorded and their DAIs were calculated. On day 14, the mice in the DSS group were sacrificed and their spleens and colons were collected. The distal colon was cut into 2–3 pieces for PAS staining and RNA isolation. Total RNA was extracted from the colon samples and 1 μg of RNA was reverse-transcribed. Real-time PCR analysis was conducted by mixing cDNAs with pairs of primers. Samples were amplified for 45 cycles and subject to the thermal cycler protocol at 95℃ for 30 sec, 58–61°C for 30 sec, and 72℃ for 40 sec. *β-actin* was used as the endogenous control gene for normalization. Finally, gene expression levels were calculated.

* $P < 0.05$, ** $P < 0.01$, *** $P < 0.005$. Analyses were performed using a Mann-Whitney U test or a one-way ANOVA with Tukey's posttest.

16. mRNA expression in DNBS-induced colitis models

Real-time PCR was performed to understand the genetic etiology of *B. breve* involved in DNBS-induced colitis models (Fig. 17). The expressions of *Notch* and *Wnt3* were greater in the DNBS-*B. breve* group than in the DNBS-vehicle group. This result may have been a non-specific response to intestinal injuries caused by DNBS. The expressions of *Spdef* and *Klf4*, which are associated with the terminal differentiation of goblet cells, and mRNA levels of *Occludin*, a membrane tight junction protein, were higher in the DNBS-*B. breve* group than in the DNBS-vehicle group. The expression of *Muc2*, which is associated with mucin secretion by goblet cells, was not higher in the DNBS-*B. breve* group than in the DNBS-vehicle group, but the expression of *Muc5* was. In these models, DNBS was administered intrarectally and sacrifice occurred five days later. Changes in colon length, body weight, DAI, and histopathologic scores indicated that mild to moderate inflammation was induced. In addition, IL-13 expression was higher in the DNBS-*B. breve* group than in the DNBS-vehicle group while IL-33 expression was not, which was consistent with a previous study.[49] The mRNA expression of *Foxo3*, a marker of butyrate metabolism, was measured because butyrate stimulates goblet cell differentiation by increasing the expression of *Klf4*. *Foxo3* expression was higher in the DNBS-*B. breve* group than in the DNBS-vehicle group.[50,51]

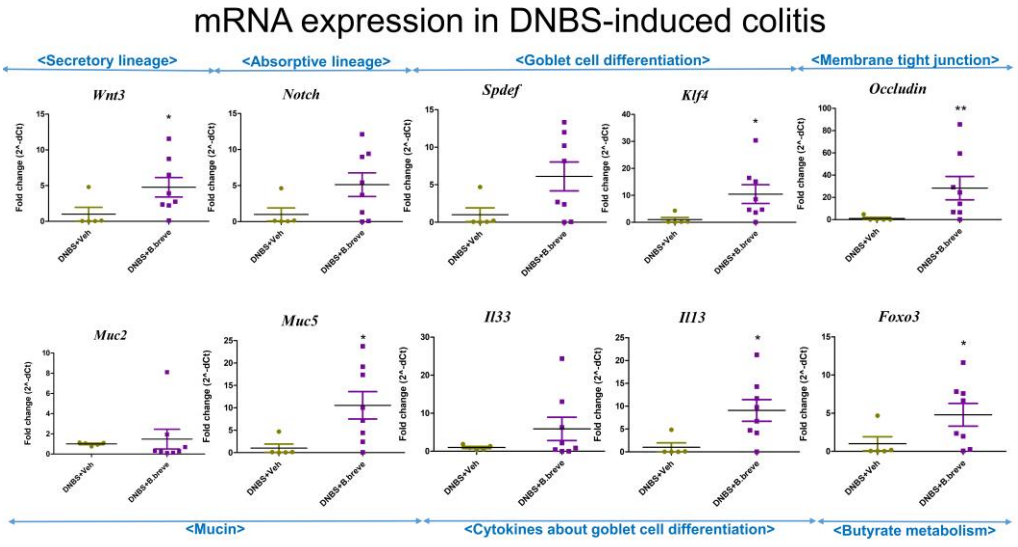

Figure 17. mRNA expression in DNBS-induced colitis models.

For the DNBS colitis experiment, 8-week-old C57BL/6 mice that weighed 20–22 g were administered 5–6mg of DNBS/100 μl with 50% ethanol rectally through a catheter. Then they were administered either 1×109 bacteria or PBS by oral gavage daily for 4 days. Daily changes in the mice were recorded and their DAIs were calculated. On day 5, the mice in the DNBS group were sacrificed and their spleens and colons were collected. The distal colon was cut into 2–3 pieces for periodic acid-Schiff staining and RNA isolation. Total RNA was extracted from the colon samples and 1 μg of RNA was reverse-transcribed. Real-time PCR analysis was conducted by mixing cDNAs with pairs of primers. Samples were amplified for 45 cycles and subject to the thermal cycler protocol at 95℃ for 30 sec, 58–61°C for 30 sec, and 72℃ for 40 sec. *β-actin* was used as the endogenous control gene for normalization. Finally, gene expression levels were calculated.

* $P < 0.05$, ** $P < 0.01$, *** $P < 0.005$. Analyses were performed using a Mann-Whitney U test or a one-way ANOVA with Tukey's posttest.

**** One case in the DNBS-*B. breve* group was not included in the analysis because it was an extreme outlier.

17. FACs analysis in *Rag1* KO mice

FACs analysis showed that the mean fluorescence of CD3-CD25-CD127+Rorgt+ILC3 was higher in male *Rag1* KO mice (Fig. 18). The male *Rag1* KO mice These mice had no mature T or B lymphocytes, which indicates that CD3-CD25-CD127+Rorgt+ILC3 may be involved in the etiology of the anti-inflammatory effects of *B. breve*.

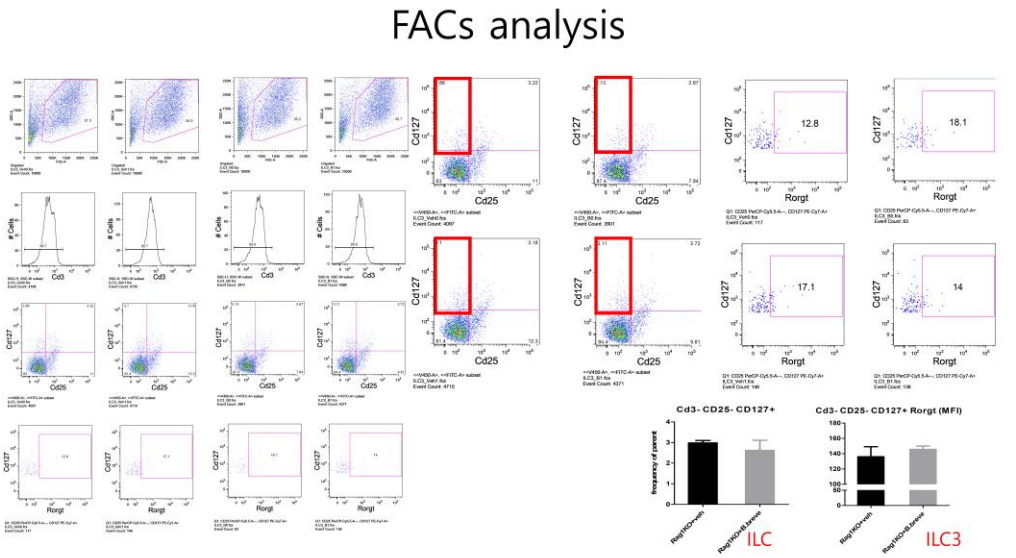

Figure 18. FACs analysis in *Rag1* KO male mice.

A total of 4 in 9-week-old male mice were administered 1×10^9 CFU of *B. breve* CBT BR3 in 0.2 mL PBS by oral gavage once per day for 6 days at which point they were sacrificed. Their spleens were dissected and splenocyte suspensions were prepared. Flow cytometric analysis of ILCs was conducted by blocking them with 2.5% normal mouse and rat serum in FACs buffer, which was composed of DPBS containing 0.1% BSA, and stained with the appropriate antibodies. The antibodies used were anti-Cd3 (eFlour 450), anti-Cd25 (PerCP-Cy5.5), anti-Cd127 (PE-Cy7), and anti-Rorgt (APC). Data was acquired using a FACSVerse flow cytometer (BD Biosciences) and analyzed using FlowJo software (Three Star, San Carlos, CA, USA).

18. In vitro Caco-2 FITC-dextran flux permeability assay

In vitro Caco-2 FITC-dextran membrane permeability tests were performed to evaluate the effect of *B. breve* on intestinal mucosal damage induced by TNF-α and associated genes involved in intestinal epithelial regeneration (Fig. 19). However, for mice whose membrane integrity was similar or better following *B. breve* administration than that of the TNF-α control group, *Occludin* and *Muc2* were more highly expressed than *Klf4*.

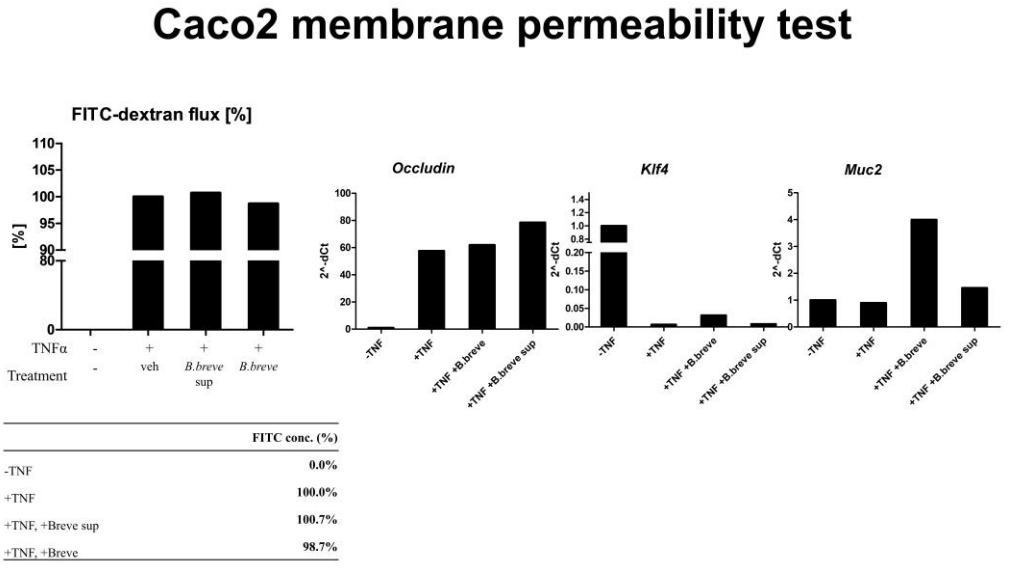

	FITC conc. (%)
-TNF	0.0%
+TNF	100.0%
+TNF, +Breve sup	100.7%
+TNF, +Breve	98.7%

Figure 19. In vitro Caco-2 FITC-dextran flux permeability assay.

FITC-dextran flux was measured to evaluate the integrity of the tight junction barriers in Caco-2 cells taken from human colon adenocarcinoma cell lines. Caco-2 cells were seeded in the upper chamber of 12-well trans-well chambers and cultured in complete Dulbecco's Modified Eagle Medium (HyClone, UT, USA), which contained 10% FBS and 1% penicillin-streptomycin, at 37℃ in a humidified atmosphere of 5% CO_2. Then 200 μl of 1 mg/ml of FITC-dextran was added to the upper chamber. After 2 h, medium from the lower chamber was collected and its fluorescence was measured using a fluorescent microplate reader. Total RNA from transwell epithelial cells was extracted and 1 μg of RNA was reverse-transcribed. Real-time PCR was conducted by mixing cDNAs with pairs of primers. Samples were amplified for 45 cycles and subject to the thermal cycler protocol at 95℃ for 30 s, 58–61℃ for 30 sec, and 72℃ for 40 sec. *β-actin* was used as the endogenous control gene for normalization. Finally, gene expression levels were calculated.

IV. Discussion

In this study, I evaluated the anti-inflammatory effects of a specific strain of probiotics using *B. breve* CBT BR3 in two experimental murine colitis models.[33,52] Few strains of *B. breve* are effective in ameliorating intestinal inflammation in murine colitis models but its pathophysiology is not fully understood although its main mechanism appears to be immunomodulation through regulatory T cells and IL-10.[53-57]

B. breve UCC2003 in neonatal mice modulates the intestinal barrier function by programming the transcriptome of intestinal epithelial cells to increase goblet cell numbers and mucus production.[58] *B. breve* M1- and M2-ameliorated murine colitis models induced by DSS by producing conjugated linoleic acid. They maintained their intestinal epithelial barriers by inhibiting inflammatory cytokine activity and modulating gut microbiota.[59] Linoleic acid, which is toxic to many bacteria, and *B. breve* DSM 20213 survived by modifying metabolism in response to linoleic acid.[60]

Additionally, *B. breve*'s exopolysaccharide may have prevented dendritic cells from maturing and activating CD4+ T cells' responses to antigens. In this way, they could evade adaptive immunity to become commensal microbiota.[61]

Although, in human studies, *B. breve* Yakult has not been shown to improve clinical outcomes in patients with ulcerative colitis, recently *B. breve* Bif195 showed protective effects against mucosal injury induced by aspirin in human small intestines. However, the pathophysiology of its anti-inflammatory effects is not clearly understood.[45,62]

In this study, I examined how *B. breve* affected two kinds of mice colitis models. DSS is one of the most frequently used chemical agents to induce colitis and it works by injuring the intestinal epithelium. DNBS causes Th-1-driven intestinal transmural inflammation. DNBS is cheaper, it triggers colitis more rapidly, and causes more consistent localized damage to the colon than DSS although DNBS requires anesthesia for rectal administration.

For the DSS-induced colitis models, the DSS-*B. breve* group had significantly better colitis symptoms in terms of DAI score, preserved body weight, colon length, colon

length-to-body weight ratio, survival rates, and histopathological scores than the DSS-vehicle group.

On the other hand, in the DNBS-colitis models, there was no significant difference between DNBS-*B. breve* and DNBS-vehicle groups in terms of these colitis symptom metrics. Of interest, it seems that DNBS definitely induced intestinal inflammation based on worse histopathological scores both in DNBS-vehicle and DNBS-*B. breve* groups. The colon inflammation in the DNBS-induced colitis group was mild on the day of sacrifice, which was 5 days after they were administered DNBS. However, 5 days may not have been long enough to trigger severe colon inflammation through the Th1 pathway.

In this study, in DSS-induced colitis model, DSS-*B. breve* group was effective than DSS-vehicle group especially in proliferating of goblet cells. Similarly, for the DNBS-induced colitis models, although there was no control group, the DNBS-*B. breve* consistently showed an augmentation in proliferating goblet cells than the DNBS-vehicle group. In both colitis models, the groups that were administered *B. breve* had higher goblet cell densities and numbers per crypt than those that were not. Of interest, *B. breve* did not have any effect in proliferating goblet cells in non-colitis group (control vs. *B. breve* without chemical-induced colitis). Taken together, these results indicate that *B. breve* is effective at regenerating goblet cells in injured mucosal layers, not in normal mucosa layers. In other words, although goblet cells proliferated in both DSS-vehicle and DSS-*B. breve* groups, they proliferated more in the DSS-*B. breve* group. In this study, intestinal mucosal injury was induced by DSS administration on days 1–7 and goblet cell counts regenerated on days 7–14, suggesting *B. breve*'s treatment effects. However, in another study, 4 strains of *B. breve* (M1, M2, M3 and M4) were administered daily for 14 days and DSS was administered on days 7–14 with goblet cell proliferation in M1, M2 but not in M3, M4 suggesting *B. breve*'s specific strains' protective effects on goblet cell loss.[59]

Goblet cell proliferation in response to mucosa injury helps prevent inflammation and controls infection by regulating the mucus layer.[63] OASIS under ER stress and *Spdef*

promote the terminal differentiation of goblet cells.[64] Goblet cells are differentiated from Lgr5+ intestinal stem cells in intestinal crypts and move from the base of the crypt to the villus over 3–6 days.[63,65] Goblet cell differentiation seems to depend on various kinds of signals. Goblet cells continuously secrete and replenish mucus into the intestinal mucosa through mucin gene expression. Although the role of mucus is not well understood, it could physically, chemically, and immunologically protect intestinal mucosa.[63,66]

Additionally, some bacteria in the outer mucus layer ferment dietary fiber into short-chain fatty acids that are used as fuel for intestinal epitheliums.[67,68] Butyrate is a short-chain fatty acid that is produced by probiotics and controls inflammation by causing bacteria to modulate macrophages, regulatory T cells, and IL-10. Butyrate also increases the number of goblet cells by increasing *Klf4* expression.[50] Therefore, butyrate may be involved in the goblet cell proliferation pathway directly or indirectly. In this study, *Foxo3*, which is directly associated with butyrate metabolism, was significantly higher in the groups that were administered *B. breve* than the groups that were not. Thus, butyrate, a microbial metabolite, may be involved in the etiology of goblet cell proliferation through *B. breve*. In addition, *B. breve* increases the mRNA expression of *Occludin* which is a membrane tight junction protein, which indicates that *B. breve* may also have a membrane-stabilizing effect.

Among four types of intestinal epithelium, namely absorptive enterocytes, goblet cells, Paneth cells, and enteroendocrine cells, *Notch* signals the differentiation of enterocyte and *Wnt* signals the differentiation of secretory lineages.[65] In this study, both *Wnt3* and *Notch* expression were higher in groups that were administered *B. breve* than in those that were not. Studies have shown that *Notch* inhibition causes epithelial progenitor cells to differentiate into goblet cells,[69,70] but in this study, *Notch* mRNA expression was higher in groups that were administered *B. breve* than those that were not. In a controlled environment, *Notch* signal inhibition might stimulate the development of secretory lineages, such as goblet cells. In this study, *Notch* signals might be non-specifically increased by *B. breve* to compensate for extensive mucosa injury induced

by DSS and DNBS, though *Notch* signal activation might not be associated with goblet cell differentiation.

In this study, IL-13 was higher in groups that were administered *B. breve* than in other groups rather than IL-33. IL-33 indirectly induces goblet cell hyperplasia through IL-13.[49] Similarly, IL-33 restores goblet cell numbers by switching macrophages' types.[71,72] Steroid receptor coactivator-3 promotes goblet cell differentiation by upregulating transcription factor *Klf4*.[73] In this study, the expressions of *Klf4* and *Spdef*, which are required for the terminal differentiation of goblet cells, were higher in both DSS and DNBS colitis models.[74]

In both colitis models, mRNA expressions of *Muc5* were higher in the groups that were administered *B. breve* than those that were not. In contrast, the expression of *Muc2*, which is necessary for *Muc2* mucus protein production, was unaffected in either colitis group. It is unclear why *Muc2* and *Muc5* can be independently activated, though goblet cells in different stages of development might be stimulated by different kinds of mucin genes. Mice with deleted *Muc2* had similar numbers of goblet cells as mice with *Muc2*, though the shape of the former group's goblet cells was not typical signifying that *Muc2* is more associated with the function of goblet cells rather than the differentiation of them.

Recently, there was a report about the genes involved in goblet cell differentiation.[75] Endoplasmic reticulum membrane protein complex subunit 3 (EMC3) is required for the differentiation and functioning of exocrine secretory lineages, such as goblet cells and Paneth cells. Deleting EMC3 causes endoplasmic reticulum (ER) stress. ER stress leads to decreased mucus production in goblet cells and Paneth cells, which in turn triggers gut microbial dysbiosis, which in turn aggravates intestinal inflammation and increases susceptibility to DSS. EMC3 depletion is associated with a relative increase in *Klf4* and decrease in *Muc2* mRNA expression, which were similarly observed in DSS-induced colitis models of this study. In other words, during goblet cell differentiation, given the increase in mRNA expression of goblet cell differentiation markers, such as *Spdef* and *Klf4*, a decrease in the mRNA expression of goblet cell

functional marker, *Muc2*, might be expected. Regardless of *Muc2* expression, *Muc5* expression levels increase during the active phase of ulcerative colitis and *Muc5* knockout-induced aggravation of inflammation, suggesting that *Muc5* may have a protective effect against colitis.[76]

Previous studies on *B. breve* and goblet cells have shown that *B. breve* may promote the differentiation of goblet cells through innate lymphoid cells and cytokines. Intestinal inflammation causes the release of cytokines such as IL-33, thereby activating innate lymphoid cells. ILC2 also secrets cytokines such as IL-13 and IL-10 that help goblet cells to differentiate.[77-80] In this study, FACs analysis showed increased mean fluorescence of $CD3^-CD25^-CD127^+Rorgt^+$ILC3 in male *Rag1* KO mice that were administered *B. breve*. No mature T or B lymphocytes were found in these mice, suggesting that $CD3^-CD25^-CD127^+Rorgt^+$ ILC3 may be involved in the etiology of the anti-inflammatory effects of *B. breve*. Based on previous studies about how *B. breve* may have anti-inflammatory effects through regulatory T cells and IL-10, *B. breve* may induce goblet cell differentiation through innate lymphoid cells and IL-10.[55,56,77,79-83]

In addition, *B. breve* SK134 showed immunomodulatory effects in the colon through $CD103^+CD11b^+$ dendritic cells in a study about immunomodulatory effects of each of the 53 human-resident bacterial species on the host immune system.[84] *B. breve* may stimulate goblet cell differentiation through intestine-specific $CD103^+CD11b^+$ dendritic cells, especially in the early phase of inflammation.[84-86]

In vitro Caco-2 FITC-dextran membrane permeability tests revealed that membrane integrity and function were higher in groups that were administered *B. breve* than in those that were not as evidenced by increased mRNA expression of mucosa barrier genes, such as *Occludin* and *Muc2*.

Goblet cells play an important role in maintaining and restoring the homeostasis of mucosa barrier functioning and may have paracrine effects through mucus. Probiotics such as *B. breve* may help augment goblet cell regeneration and hyperplasia, especially in the face of mucosal injury. Intestinal epithelial barrier dysfunction is a key part of

IBD pathogenesis, so probiotics such as *B. breve* may play a significant role in ameliorating mucosal inflammation by assisting goblet cell regeneration.

V. Conclusion

Bifidobacterium breve CBT BR3 is effective in relieving intestinal inflammation by augmenting goblet cell regeneration.

References

1. Isolauri E, Kirjavainen PV, Salminen S. Probiotics: a role in the treatment of intestinal infection and inflammation? Gut 2002;50 Suppl 3:III54-9.
2. Wasilewski A, Zielinska M, Storr M, Fichna J. Beneficial Effects of Probiotics, Prebiotics, Synbiotics, and Psychobiotics in Inflammatory Bowel Disease. Inflamm Bowel Dis 2015;21:1674-82.
3. Isolauri E, Salminen S, Ouwehand AC. Microbial-gut interactions in health and disease. Probiotics. Best Pract Res Clin Gastroenterol 2004;18:299-313.
4. Saito Y, Hinoi T, Adachi T, Miguchi M, Niitsu H, Kochi M, et al. Synbiotics suppress colitis-induced tumorigenesis in a colon-specific cancer mouse model. PLoS One 2019;14:e0216393.
5. Gorbach SL. Probiotics and gastrointestinal health. Am J Gastroenterol 2000;95:S2-4.
6. Reid G, Jass J, Sebulsky MT, McCormick JK. Potential uses of probiotics in clinical practice. Clin Microbiol Rev 2003;16:658-72.
7. Isolauri E, Sutas Y, Kankaanpaa P, Arvilommi H, Salminen S. Probiotics: effects on immunity. Am J Clin Nutr 2001;73:444S-50S.
8. Borchers AT, Selmi C, Meyers FJ, Keen CL, Gershwin ME. Probiotics and immunity. J Gastroenterol 2009;44:26-46.
9. Smelt MJ, de Haan BJ, Bron PA, van Swam I, Meijerink M, Wells JM, et al. Probiotics can generate FoxP3 T-cell responses in the small intestine and simultaneously inducing CD4 and CD8 T cell activation in the large intestine. PLoS One 2013;8:e68952.
10. Shih DQ, Kwan LY, Chavez V, Cohavy O, Gonsky R, Chang EY, et al. Microbial induction of inflammatory bowel disease associated gene TL1A (TNFSF15) in antigen presenting cells. Eur J Immunol 2009;39:3239-50.
11. Shanahan F. Probiotics and inflammatory bowel disease: is there a scientific rationale? Inflamm Bowel Dis 2000;6:107-15.
12. Chassaing B, Darfeuille-Michaud A. The commensal microbiota and enteropathogens in the pathogenesis of inflammatory bowel diseases. Gastroenterology 2011;140:1720-28.
13. Conte MP, Schippa S, Zamboni I, Penta M, Chiarini F, Seganti L, et al. Gut-associated bacterial microbiota in paediatric patients with inflammatory bowel disease. Gut 2006;55:1760-7.
14. Fedorak RN, Madsen KL. Probiotics and the management of inflammatory bowel disease. Inflamm Bowel Dis 2004;10:286-99.
15. Kruis W. Review article: antibiotics and probiotics in inflammatory bowel disease. Aliment Pharmacol Ther 2004;20 Suppl 4:75-8.
16. Sheil B, Shanahan F, O'Mahony L. Probiotic effects on inflammatory bowel disease. J Nutr 2007;137:819S-24S.
17. Ghouri YA, Richards DM, Rahimi EF, Krill JT, Jelinek KA, DuPont AW. Systematic review of randomized controlled trials of probiotics, prebiotics,

and synbiotics in inflammatory bowel disease. Clin Exp Gastroenterol 2014;7:473-87.
18. Derwa Y, Gracie DJ, Hamlin PJ, Ford AC. Systematic review with meta-analysis: the efficacy of probiotics in inflammatory bowel disease. Aliment Pharmacol Ther 2017;46:389-400.
19. Prantera C, Scribano ML, Falasco G, Andreoli A, Luzi C. Ineffectiveness of probiotics in preventing recurrence after curative resection for Crohn's disease: a randomised controlled trial with Lactobacillus GG. Gut 2002;51:405-9.
20. Rembacken BJ, Snelling AM, Hawkey PM, Chalmers DM, Axon AT. Non-pathogenic Escherichia coli versus mesalazine for the treatment of ulcerative colitis: a randomised trial. Lancet 1999;354:635-9.
21. Bibiloni R, Fedorak RN, Tannock GW, Madsen KL, Gionchetti P, Campieri M, et al. VSL#3 probiotic-mixture induces remission in patients with active ulcerative colitis. Am J Gastroenterol 2005;100:1539-46.
22. Kruis W, Fric P, Pokrotnieks J, Lukas M, Fixa B, Kascak M, et al. Maintaining remission of ulcerative colitis with the probiotic Escherichia coli Nissle 1917 is as effective as with standard mesalazine. Gut 2004;53:1617-23.
23. Ishikawa H, Akedo I, Umesaki Y, Tanaka R, Imaoka A, Otani T. Randomized controlled trial of the effect of bifidobacteria-fermented milk on ulcerative colitis. J Am Coll Nutr 2003;22:56-63.
24. Fujimori S, Tatsuguchi A, Gudis K, Kishida T, Mitsui K, Ehara A, et al. High dose probiotic and prebiotic cotherapy for remission induction of active Crohn's disease. J Gastroenterol Hepatol 2007;22:1199-204.
25. Tursi A, Brandimarte G, Papa A, Giglio A, Elisei W, Giorgetti GM, et al. Treatment of relapsing mild-to-moderate ulcerative colitis with the probiotic VSL#3 as adjunctive to a standard pharmaceutical treatment: a double-blind, randomized, placebo-controlled study. Am J Gastroenterol 2010;105:2218-27.
26. Zocco MA, dal Verme LZ, Cremonini F, Piscaglia AC, Nista EC, Candelli M, et al. Efficacy of Lactobacillus GG in maintaining remission of ulcerative colitis. Aliment Pharmacol Ther 2006;23:1567-74.
27. Dotan I, Rachmilewitz D. Probiotics in inflammatory bowel disease: possible mechanisms of action. Curr Opin Gastroenterol 2005;21:426-30.
28. Hedin CR, Mullard M, Sharratt E, Jansen C, Sanderson JD, Shirlaw P, et al. Probiotic and prebiotic use in patients with inflammatory bowel disease: a case-control study. Inflamm Bowel Dis 2010;16:2099-108.
29. Whelan K, Quigley EM. Probiotics in the management of irritable bowel syndrome and inflammatory bowel disease. Curr Opin Gastroenterol 2013;29:184-9.
30. Wang W, Chen L, Zhou R, Wang X, Song L, Huang S, et al. Increased proportions of Bifidobacterium and the Lactobacillus group and loss of

butyrate-producing bacteria in inflammatory bowel disease. J Clin Microbiol 2014;52:398-406.
31. Matsumoto S, Watanabe N, Imaoka A, Okabe Y. Preventive effects of Bifidobacterium- and Lactobacillus-fermented milk on the development of inflammatory bowel disease in senescence-accelerated mouse P1/Yit strain mice. Digestion 2001;64:92-9.
32. O'Mahony L, McCarthy J, Kelly P, Hurley G, Luo F, Chen K, et al. Lactobacillus and bifidobacterium in irritable bowel syndrome: symptom responses and relationship to cytokine profiles. Gastroenterology 2005;128:541-51.
33. Tojo R, Suarez A, Clemente MG, de los Reyes-Gavilan CG, Margolles A, Gueimonde M, et al. Intestinal microbiota in health and disease: role of bifidobacteria in gut homeostasis. World J Gastroenterol 2014;20:15163-76.
34. Shiba T, Aiba Y, Ishikawa H, Ushiyama A, Takagi A, Mine T, et al. The suppressive effect of bifidobacteria on Bacteroides vulgatus, a putative pathogenic microbe in inflammatory bowel disease. Microbiol Immunol 2003;47:371-8.
35. Enomoto T, Sowa M, Nishimori K, Shimazu S, Yoshida A, Yamada K, et al. Effects of bifidobacterial supplementation to pregnant women and infants in the prevention of allergy development in infants and on fecal microbiota. Allergol Int 2014;63:575-85.
36. Kirjavainen PV, Arvola T, Salminen SJ, Isolauri E. Aberrant composition of gut microbiota of allergic infants: a target of bifidobacterial therapy at weaning? Gut 2002;51:51-5.
37. Lievin V, Peiffer I, Hudault S, Rochat F, Brassart D, Neeser JR, et al. Bifidobacterium strains from resident infant human gastrointestinal microflora exert antimicrobial activity. Gut 2000;47:646-52.
38. Kitajima H, Sumida Y, Tanaka R, Yuki N, Takayama H, Fujimura M. Early administration of Bifidobacterium breve to preterm infants: randomised controlled trial. Arch Dis Child Fetal Neonatal Ed 1997;76:F101-7.
39. Bozzi Cionci N, Baffoni L, Gaggia F, Di Gioia D. Therapeutic Microbiology: The Role of Bifidobacterium breve as Food Supplement for the Prevention/Treatment of Paediatric Diseases. Nutrients 2018;10.
40. Ohtsuka Y, Ikegami T, Izumi H, Namura M, Ikeda T, Ikuse T, et al. Effects of Bifidobacterium breve on inflammatory gene expression in neonatal and weaning rat intestine. Pediatr Res 2012;71:46-53.
41. Kwak MJ, Yoon JK, Kwon SK, Chung MJ, Seo JG, Kim JF. Complete genome sequence of the probiotic bacterium Bifidobacterium breve KCTC 12201BP isolated from a healthy infant. J Biotechnol 2015;214:156-7.
42. Sivan A, Corrales L, Hubert N, Williams JB, Aquino-Michaels K, Earley ZM, et al. Commensal Bifidobacterium promotes antitumor immunity and facilitates anti-PD-L1 efficacy. Science 2015;350:1084-9.

43. Robles-Vera I, de la Visitacion N, Toral M, Sanchez M, Romero M, Gomez-Guzman M, et al. Probiotic Bifidobacterium breve prevents DOCA-salt hypertension. FASEB J 2020;34:13626-40.
44. Lee JS, Chung MJ, Seo JG. In Vitro Evaluation of Antimicrobial Activity of Lactic Acid Bacteria against Clostridium difficile. Toxicol Res 2013;29:99-106.
45. Mortensen B, Murphy C, O'Grady J, Lucey M, Elsafi G, Barry L, et al. Bifidobacteriumbreve Bif195 Protects Against Small-Intestinal Damage Caused by Acetylsalicylic Acid in Healthy Volunteers. Gastroenterology 2019;157:637-46 e4.
46. Chassaing B, Aitken JD, Malleshappa M, Vijay-Kumar M. Dextran sulfate sodium (DSS)-induced colitis in mice. Curr Protoc Immunol 2014;104:15 25 1-15 25 14.
47. Morampudi V, Bhinder G, Wu X, Dai C, Sham HP, Vallance BA, et al. DNBS/TNBS colitis models: providing insights into inflammatory bowel disease and effects of dietary fat. J Vis Exp 2014:e51297.
48. Erben U, Loddenkemper C, Doerfel K, Spieckermann S, Haller D, Heimesaat MM, et al. A guide to histomorphological evaluation of intestinal inflammation in mouse models. International Journal of Clinical and Experimental Pathology 2014;7:4557-U27.
49. Waddell A, Vallance JE, Hummel A, Alenghat T, Rosen MJ. IL-33 Induces Murine Intestinal Goblet Cell Differentiation Indirectly via Innate Lymphoid Cell IL-13 Secretion. J Immunol 2019;202:598-607.
50. Chen J, Vitetta L. The Role of Butyrate in Attenuating Pathobiont-Induced Hyperinflammation. Immune Netw 2020;20:e15.
51. Kaiko GE, Ryu SH, Koues OI, Collins PL, Solnica-Krezel L, Pearce EJ, et al. The Colonic Crypt Protects Stem Cells from Microbiota-Derived Metabolites. Cell 2016;165:1708-20.
52. Gueimonde M, Ouwehand A, Huhtinen H, Salminen E, Salminen S. Qualitative and quantitative analyses of the bifidobacterial microbiota in the colonic mucosa of patients with colorectal cancer, diverticulitis and inflammatory bowel disease. World J Gastroenterol 2007;13:3985-9.
53. Collins JW, Akin AR, Kosta A, Zhang N, Tangney M, Francis KP, et al. Pre-treatment with Bifidobacterium breve UCC2003 modulates Citrobacter rodentium-induced colonic inflammation and organ specificity. Microbiology 2012;158:2826-34.
54. Heuvelin E, Lebreton C, Grangette C, Pot B, Cerf-Bensussan N, Heyman M. Mechanisms involved in alleviation of intestinal inflammation by bifidobacterium breve soluble factors. PLoS One 2009;4:e5184.
55. Zheng B, van Bergenhenegouwen J, Overbeek S, van de Kant HJ, Garssen J, Folkerts G, et al. Bifidobacterium breve attenuates murine dextran sodium sulfate-induced colitis and increases regulatory T cell responses. PLoS One 2014;9:e95441.

56. Jeon SG, Kayama H, Ueda Y, Takahashi T, Asahara T, Tsuji H, et al. Probiotic Bifidobacterium breve induces IL-10-producing Tr1 cells in the colon. PLoS Pathog 2012;8:e1002714.
57. Imaoka A, Shima T, Kato K, Mizuno S, Uehara T, Matsumoto S, et al. Anti-inflammatory activity of probiotic Bifidobacterium: enhancement of IL-10 production in peripheral blood mononuclear cells from ulcerative colitis patients and inhibition of IL-8 secretion in HT-29 cells. World J Gastroenterol 2008;14:2511-6.
58. Kiu R, Treveil A, Harnisch LC, Caim S, Leclaire C, van Sinderen D, et al. Bifidobacterium breve UCC2003 Induces a Distinct Global Transcriptomic Program in Neonatal Murine Intestinal Epithelial Cells. iScience 2020;23:101336.
59. Chen Y, Jin Y, Stanton C, Paul Ross R, Zhao J, Zhang H, et al. Alleviation effects of Bifidobacterium breve on DSS-induced colitis depends on intestinal tract barrier maintenance and gut microbiota modulation. Eur J Nutr 2021;60:369-87.
60. Senizza A, Rocchetti G, Callegari ML, Lucini L, Morelli L. Linoleic acid induces metabolic stress in the intestinal microorganism Bifidobacterium breve DSM 20213. Sci Rep 2020;10:5997.
61. Hickey A, Stamou P, Udayan S, Ramon-Vazquez A, Esteban-Torres M, Bottacini F, et al. Bifidobacterium breve Exopolysaccharide Blocks Dendritic Cell Maturation and Activation of CD4(+) T Cells. Front Microbiol 2021;12:653587.
62. Matsuoka K, Uemura Y, Kanai T, Kunisaki R, Suzuki Y, Yokoyama K, et al. Efficacy of Bifidobacterium breve Fermented Milk in Maintaining Remission of Ulcerative Colitis. Dig Dis Sci 2018;63:1910-9.
63. Birchenough GM, Johansson ME, Gustafsson JK, Bergstrom JH, Hansson GC. New developments in goblet cell mucus secretion and function. Mucosal Immunol 2015;8:712-9.
64. Asada R, Saito A, Kawasaki N, Kanemoto S, Iwamoto H, Oki M, et al. The endoplasmic reticulum stress transducer OASIS is involved in the terminal differentiation of goblet cells in the large intestine. J Biol Chem 2012;287:8144-53.
65. Gersemann M, Stange EF, Wehkamp J. From intestinal stem cells to inflammatory bowel diseases. World J Gastroenterol 2011;17:3198-203.
66. Cornick S, Kumar M, Moreau F, Gaisano H, Chadee K. VAMP8-mediated MUC2 mucin exocytosis from colonic goblet cells maintains innate intestinal homeostasis. Nat Commun 2019;10:4306.
67. Martini E, Krug SM, Siegmund B, Neurath MF, Becker C. Mend Your Fences: The Epithelial Barrier and its Relationship With Mucosal Immunity in Inflammatory Bowel Disease. Cell Mol Gastroenterol Hepatol 2017;4:33-46.

68. Liu Q, Yu Z, Tian F, Zhao J, Zhang H, Zhai Q, et al. Surface components and metabolites of probiotics for regulation of intestinal epithelial barrier. Microb Cell Fact 2020;19:23.
69. Zhou Y, Rychahou P, Wang Q, Weiss HL, Evers BM. TSC2/mTORC1 signaling controls Paneth and goblet cell differentiation in the intestinal epithelium. Cell Death Dis 2015;6:e1631.
70. VanDussen KL, Carulli AJ, Keeley TM, Patel SR, Puthoff BJ, Magness ST, et al. Notch signaling modulates proliferation and differentiation of intestinal crypt base columnar stem cells. Development 2012;139:488-97.
71. Seo DH, Che X, Kwak MS, Kim S, Kim JH, Ma HW, et al. Interleukin-33 regulates intestinal inflammation by modulating macrophages in inflammatory bowel disease. Sci Rep 2017;7:851.
72. Kim SW, Kim S, Son M, Cheon JH, Park YS. Melatonin controls microbiota in colitis by goblet cell differentiation and antimicrobial peptide production through Toll-like receptor 4 signalling. Sci Rep 2020;10:2232.
73. Chen W, Zhuo M, Lu X, Xia X, Zhao Y, Huang Z, et al. SRC-3 protects intestine from DSS-induced colitis by inhibiting inflammation and promoting goblet cell differentiation through enhancement of KLF4 expression. Int J Biol Sci 2018;14:2051-64.
74. Gersemann M, Becker S, Kubler I, Koslowski M, Wang G, Herrlinger KR, et al. Differences in goblet cell differentiation between Crohn's disease and ulcerative colitis. Differentiation 2009;77:84-94.
75. Huang M, Yang L, Jiang N, Dai Q, Li R, Zhou Z, et al. Emc3 maintains intestinal homeostasis by preserving secretory lineages. Mucosal Immunol 2021;14:873-86.
76. Olli KE, Rapp C, O'Connell L, Collins CB, McNamee EN, Jensen O, et al. Muc5ac Expression Protects the Colonic Barrier in Experimental Colitis. Inflamm Bowel Dis 2020;26:1353-67.
77. Bando JK, Gilfillan S, Di Luccia B, Fachi JL, Secca C, Cella M, et al. ILC2s are the predominant source of intestinal ILC-derived IL-10. J Exp Med 2020;217.
78. Eberl G, Colonna M, Di Santo JP, McKenzie AN. Innate lymphoid cells. Innate lymphoid cells: a new paradigm in immunology. Science 2015;348:aaa6566.
79. Grondin JA, Kwon YH, Far PM, Haq S, Khan WI. Mucins in Intestinal Mucosal Defense and Inflammation: Learning From Clinical and Experimental Studies. Front Immunol 2020;11:2054.
80. Klose CSN, Artis D. Innate lymphoid cells control signaling circuits to regulate tissue-specific immunity. Cell Res 2020;30:475-91.
81. Sun H, Wu Y, Zhang Y, Ni B. IL-10-Producing ILCs: Molecular Mechanisms and Disease Relevance. Front Immunol 2021;12:650200.
82. Jenkins BR, Blaseg NA, Grifka-Walk HM, Deuling B, Swain SD, Campbell EL, et al. Loss of interleukin-10 receptor disrupts intestinal epithelial cell

proliferation and skews differentiation towards the goblet cell fate. FASEB J 2021;35:e21551.
83. Hasnain SZ, Tauro S, Das I, Tong H, Chen AC, Jeffery PL, et al. IL-10 promotes production of intestinal mucus by suppressing protein misfolding and endoplasmic reticulum stress in goblet cells. Gastroenterology 2013;144:357-68 e9.
84. Geva-Zatorsky N, Sefik E, Kua L, Pasman L, Tan TG, Ortiz-Lopez A, et al. Mining the Human Gut Microbiota for Immunomodulatory Organisms. Cell 2017;168:928-43 e11.
85. Bain CC, Montgomery J, Scott CL, Kel JM, Girard-Madoux MJH, Martens L, et al. TGFbetaR signalling controls CD103(+)CD11b(+) dendritic cell development in the intestine. Nat Commun 2017;8:620.
86. McDole JR, Wheeler LW, McDonald KG, Wang B, Konjufca V, Knoop KA, et al. Goblet cells deliver luminal antigen to CD103+ dendritic cells in the small intestine. Nature 2012;483:345-9.

ABSTRACT (IN KOREAN)

Bifidobacterium breve CBT BR3의 술잔 세포 증식 촉진을 통한 장 염증 개선효과

<지도교수 천재희>

연세대학교 대학원 의학과

유종욱

유산균은 숙주에 이로운 효과를 주는 미생물로 이중 *Bifidobacterium*은 혐기성, 그램 양성, 카탈라제 음성인 간균이다. *Bifidobacterium*의 다양한 종 중에서 *Bifidobacterium breve*는 건강한 영아에서 잘 분리되는 박테리아로 모유수유를 한 영아에서 우세한 균주로 알려져 있다. *Bifidobacterium breve*의 일부 계통으로 시행된 동물 및 인간 연구에서 장 염증에 효과가 있었으나, 기전이 명확하지 않아, 이 연구에서는 실험 동물 모델을 통해 그 기전을 연구하고자 한다. *Bifidobacterium breve* CBT BR3가 두가지 동물 장 염증 모델, 즉 DSS 및 DNBS로 장 염증이 유도된 마우스 모델에 경구 투여되었고, 질병 활동성 지수(disease activity index)를 추적 관찰하였다. 또한 부검을 통해 장 조직을 채취 후 조직 병리, PAS 염색, goblet cell 밀도 및 mRNA 표현을 통해서 분석하였다. 그 결과 DSS 마우스 모델에서는 장 염증 증상 및 생존율이 개선되었고, 체중, 장 길이, 장 길이/초기 체중이 보존되었다. 또한 DSS, DNBS 모델 모두에서 현미경적,

조직학적으로 술잔 세포 숫자의 증가를 확인할 수 있었다. mRNA 분석 결과 DSS, DNBS 모델 모두에서 술잔 세포 분화와 연관된 *Klf4, Spdef*가 증가한 반면 mucin분비와 연관된 *Muc5*는 증가하였으나 반면 *Muc2*는 증가하지 않았다. 반면 DNBS 모델에서는 장내 미생물의 metabolite인 butyrate의 metabolism과 연관된 *Foxo3* 및 막 밀착 연접에 연관된 유전자인 *Occludin*의 발현이 모두 증가하였다. 또한 *Rag1* KO 마우스에서 FACs 분석 결과, innate lymphoid cell이 *B. breve* 투여와 상관 관계가 있었다. 이상의 연구결과를 통해 *Bifidobacterium breve* CBT BR3가 butyrate metabolism 혹은 innate lymphoid cell과 연관된 경로를 통해 유전자 발현 촉진을 통해 술잔 세포 증식을 촉진하여 장 염증 개선 효과를 나타냄을 확인할 수 있었다.

핵심 되는 말: 염증성 장 질환, 술잔 세포, 유산균, *Bifidobacterium breve*, innate lymphoid cells